Reprinted from: COENOSES 11: 77 - 100 (1996)

Fractals in the Biological Sciences

N.C. Kenkel and D.J. Walker
Department of Botany
University of Manitoba
Winnipeg R3T 2N2
Canada
kenkel@cc.umanitoba.ca
djwalkr@cc.umanitoba.ca

Abstract

The importance of spatial and temporal scaling to the study of biological systems and processes has long been recognized. We demonstrate that concepts derived from fractal and chaos theory are fundamental to the description and modelling of scale-related phenomena in biology, from the molecular to ecosystem levels of organization. Algorithms for estimating the fractal dimension are described, and numerous applications of fractal theory in the biological sciences are summarized.

Keywords

chaos theory; fractal theory; multifractals; scale-invariance; self-similarity; spatial pattern.

1. INTRODUCTION

1.1 Fractal and Euclidean Geometries

Western culture is obsessed with order, smoothness and symmetry, to the point that we often impose on nature patterns and models derived from classical Greek geometry. Historically this tendency can be traced to Plato, for whom the 'real' world consisted of smooth, Euclidean shapes created by a supreme being. By contrast, the world we inhabit was created by a lesser, demiurgical being, and is nothing more than a rough, asymmetrical copy of the 'real' world. According to Plato, the 'real' world can only be glimpsed occasionally through the mind. In this way, Plato was able to reconcile the inability of classical geometry (as later formulated by Euclid) to describe the world we inhabit. Peters (1994) has described fractal geometry as that of the Demiurge.

Despite the fact that Euclidean geometry is a gross simplification of the world, western society has tenaciously clung to this ordered view. Such a view divorces us from nature, since we tend to perceive deviations from symmetry as fundamentally wrong, as something to be corrected. This is learned very early, for example when children are taught to represent complex natural objects such as trees as simple Euclidean constructs (e.g. triangles, circles, rectangles). In later life, we expend considerable effort creating and maintaining symmetric patterns in our gardens (Victorian topiary being an extreme example). Our architecture also reflects these deeply ingrained traditions of symmetry and order: a good early example is the Roman Pantheon, which incorporates three basic shapes of Euclidean geometry (the circle, triangle, and rectangle). More modern examples include the palaces of the French kings, the fascist architecture of Germany and Italy, and indeed any modern city skyline. It is instructive to note that human-made objects invariably stand out against the natural, more 'fractal' world.

1.2 What is Fractal Geometry?

Mandelbrot (1975) introduced the term 'fractal' (from the latin fractus, meaning 'broken') to characterize spatial or temporal phenomena that are continuous but not differentiable. Unlike more familiar Euclidean constructs, every attempt to split a fractal into smaller pieces results in the resolution of more structure. Fractal objects and processes are therefore said to display 'self-invariant' (self-similar or self-affine) properties (Hastings and Sugihara 1993). Self-similar objects are isotropic upon rescaling, whereas rescaling of self-affine objects is direction-dependent (anisotropic). Thus the trace of particulate Brownian motion in two-dimensional space is self-similar, whereas a plot of the x-coordinate of the particle as a function of time is self-affine (Brown 1995).

Fractal properties include scale independence, self-similarity, complexity, and infinite length or detail. Fractal structures do not have a single length scale, while fractal processes (time series) cannot be characterized by a single time scale (West and Goldberger 1987). Nonetheless, the necessary and sufficient conditions for an object (or process) to possess fractal properties have not been formally defined. Indeed, fractal geometry has been described as "a collection of examples, linked by a common point of view, not an organized theory"

(Lorimer et al. 1994).

Fractal theory offers methods for describing the inherent irregularity of natural objects. In fractal analysis, the Euclidean concept of 'length' is viewed as a process. This process is characterized by a constant parameter D known as the fractal (or fractional) dimension. The fractal dimension can be viewed as a relative measure of complexity, or as an index of the scale-dependency of a pattern. Excellent summaries of basic concepts of fractal geometry can be found in Mandelbrot (1982), Frontier (1987), Schroeder (1991), Turcotte (1992), Hastings and Sugihara (1993), Lam and De Cola (1993) and in many of the references cited below.

The fractal dimension is a summary statistic measuring overall 'complexity'. Like many summary statistics (e.g. mean), it is obtained by 'averaging' variation in data structure (Normant and Tricot 1993). In doing so, information is necessarily lost. The estimated fractal dimension of a lakeshore, for example, tells us nothing about the actual size or overall shape of the lake, nor can we reproduce a map of the lake from D alone. However, the fractal dimension does tell us a great deal about the relative complexity of the lakeshore, and as such is an important descriptor when used in conjunction with other measures.

1.3 Fractals in the Biological Sciences

Biologists have traditionally modelled nature using Euclidean representations of natural objects or series. Examples include the representation of heart rates as sine waves, conifer trees as cones, animal habitats as simple areas, and cell membranes as curves or simple surfaces. However, scientists have come to recognize that many natural constructs are better characterized using fractal geometry. Biological systems and processes are typically characterized by many levels of substructure, with the same general pattern being repeated in an ever-decreasing cascade. Relationships that depend on scale have profound implications in human physiology (West and Goldberger 1987), ecology (Loehle 1983; Wiens 1989), and many other sub-disciplines of biology. The importance of fractal scaling has been recognized at virtually every level of biological organization (**Fig. 1**; **Section 5**).

Fractal geometry may prove to be a unifying theme in biology (Kenkel and Walker 1993), since it permits generalization of the fundamental concepts of dimension and length measurement. Most biological processes and structures are decidedly non-Euclidean, displaying discontinuities, jaggedness, and fragmentation. Classical measurement and scaling methods such as Euclidean geometry, calculus and the Fourier transform assume continuity and smoothness. However, it is important to recognize that while Euclidean geometry is not realized in nature, neither is strict mathematical fractal geometry. Specifically, there is a lower limit to self-similarity in most biological systems, and nature adds an element of randomness to its fractal structures. Nonetheless, fractal geometry is far closer to nature than is Euclidean geometry (Deering and West 1992).

The relevance of fractal theory to biological problems is dependent on objectives. To the forester interested in estimating stand board-feet, a Euclidean representation of a tree trunk (as a cylinder or elongated cone) may be quite adequate. However, for an ecologist interested in modelling habitat availability on tree trunks (say, for small epiphytes or invertebrates), fractal geometry is more appropriate. Using a fractal approach, the complex surface of tree bark is readily quantified. A forester's diameter tape ignores the surface roughness of the bark, giving but a crude estimate of the circumference of the trunk. For an insect 10 mm in length, the 'distance' that it must travel to circumnavigate the trunk is much greater than the measured diameter value. For an insect of length 1 mm, the distance travelled is greater still. This has consequences on the way that the tree trunk is perceived by organisms of different sizes. If the bark has a fractal dimension of D = 1.4, an insect an order of magnitude smaller than another perceives a length increase of $10^{D-1} = 10^{0.4} = 2.51$, or a habitat surface area increase of $2.5^{1.2} = 6.31$. By contrast, for a smooth Euclidean surface, D = 1 and both insects perceive the same 'amount' of habitat. The higher the fractal dimension D, the greater the perceived rate of increase in length (or surface) with decreasing scale.

2. THE FRACTAL DIMENSION

Formally, a mathematical fractal is defined as any series for which the Hausdorff dimension (a continuous function) exceeds the discrete topological dimension (Tsonis and Tsonis 1987). Topologically, a line is one-dimensional. The dimension D of a fractal 'trace' on the plane, however, is a continuous function with range $1 \leq D \leq 2$. A completely differentiable series has a fractal dimension D = 1 (the same as the topological dimension), while a Brownian trace completely occupies two-dimensional topological space and therefore has a fractal dimension D = 2. Fractal dimensions $1 \leq D \leq 2$ quantify the degree to which a trace 'fills' the plane. In

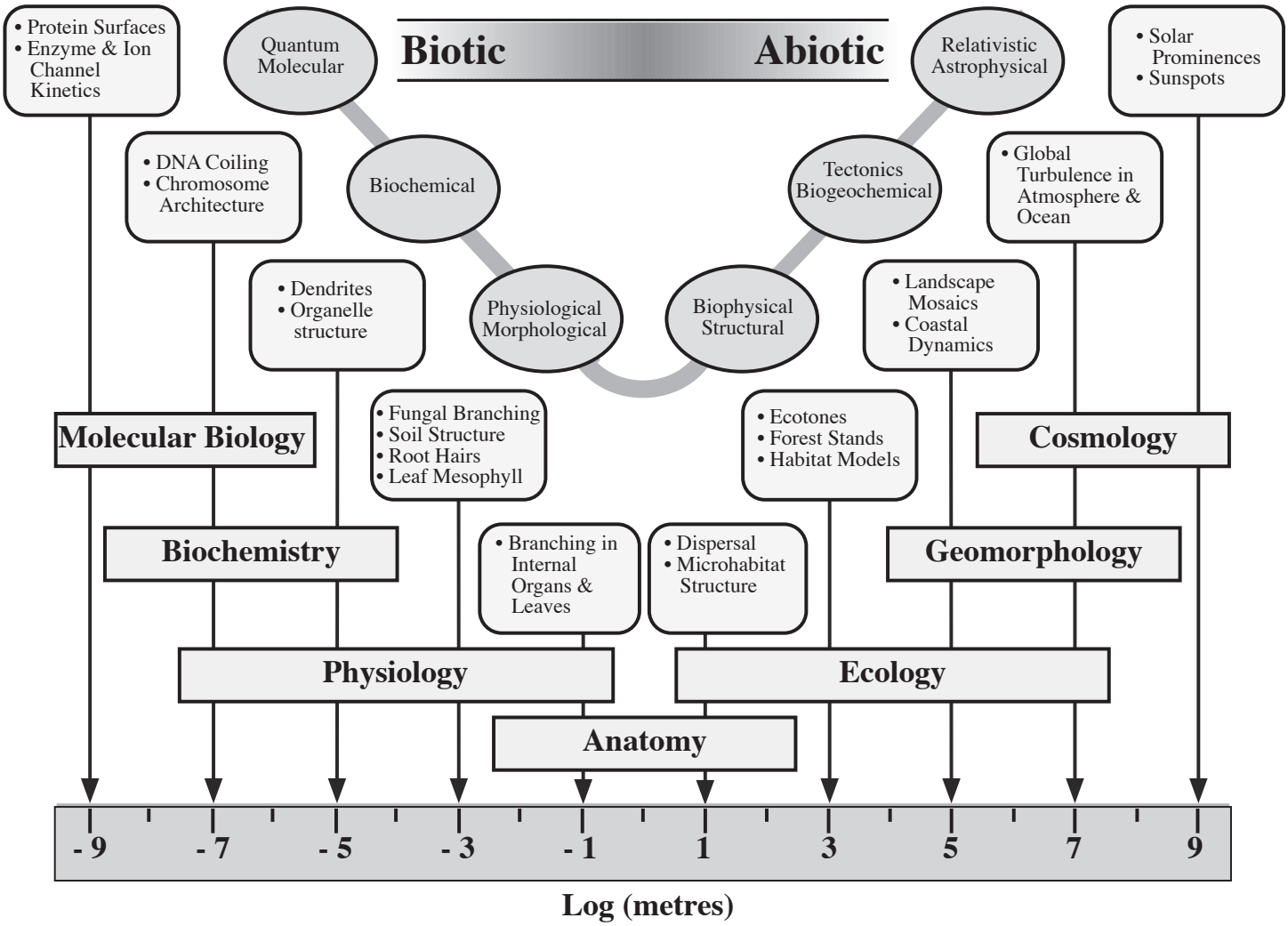

Fig. 1. Examples of fractal patterns at various spatial scales (rounded boxes). Ovals summarize general processes operating at each scale: biotic processes predominate at finer spatial scales, abiotic processes at coarser scales. Rectangles indicate the scientific disciplines at which these patterns and processes are normally studied.

the same way, a planar curved surface is topologically two-dimensional, while a fractal surface has dimension $2 \leq D \leq 3$.

Consider estimation of the length of a complex 'coastline'. For a given spatial scale δ, the total length Lδ is estimated as a set of N straight-line segments of length δ. Because small 'peninsulas' and other features not recognized at coarser scales become apparent at finer scales, the measured length Lδ increases as δ decreases (Mandelbrot 1967). This dependence of length on measurement scale is a fundamental feature of fractal objects. The relationship between length and measuring scale is summarized by the power law:

$$L\delta = K\delta - D \qquad [1]$$

where K is a constant. The fractal dimension ($1 \leq D \leq 2$) quantifies the degree of coastline complexity. In practice, D can be estimated from the slope of the log-log plot:

$$\log L\delta = \log K + (1 - D)\log \delta \qquad [2]$$

Note that the measured length is independent of measurement scale (D = 1) for Euclidean (non-fractal) objects.

Mathematical fractals exhibit exact self-similarity across all spatial or temporal scales, such that successive magnifications reveal an identical structure. An example is the Koch 'curve' (Sugihara and May 1990; Schroeder 1991: 8), a fractal object in which a reduction in the measuring scale by one-third (δn+1/δn = 1/3) increases the measured length by four-thirds (Ln+1/Ln) = 4/3. Substituting into the power law relationship:

$(Ln+1/Ln) = (\delta n+1/\delta n)1\text{-}D$

$(4/3) = (1/3)1\text{-}D$

$4 = 3D$

$D = \log 4/\log 3 = 1.26.$

Unlike mathematical fractals, natural objects do not

display exact self-similarity. Nevertheless, many natural objects do display some degree of 'statistical' self-similarity, at least over a limited range of spatial or temporal scales. For example, lung branching shows statistical self-similarity over 14 dichotomies, and trees branching over 8 dichotomies (Lorimer et al. 1994). Statistical self-similarity refers to scale-related repetitions of overall complexity, but not of the exact pattern. Specifically, details at a given scale are similar, though not identical, to those seen at coarser or finer scales. It should be emphasized, however, that statistical self-similarity is not a prerequisite to applying fractal theory. Normant and Tricot (1993) emphasize this point:

> "... a geographical line is seen as a fairly nonhomogeneous curve, that is, with both straight lines (almost recifiable) and chaotic parts, whose local dimension is not the same everywhere. Such curves are not self-similar, not even statistically ... it is necessary to stress the fact that fractal does not imply self-similar, and thus coastlines are not self-similar, but fractal ... we assert that self-similarity is a restrictive point of view".

The fractal dimension D is most commonly estimated from the regression slope of a log-log power law plot. However, the definition of 'independent' and 'dependent' variables (required in least squares or Model I regression analysis) is not straightforward in such applications (Zeide and Gresham 1991). This is a serious but largely unrecognized problem, for using least square regression in this way results in a biased slope estimate (Kenkel and Walker 1993; Loehle and Bai-Lian 1995). Model II regression analysis should be used instead. Two methods, principal axis regression (equivalent to principal components analysis) and reduced major axis regression, are available. The reduced major axis slope is obtained very simply, as the least squares (Model I) slope divided by the product-moment correlation between the two variables (Niklas 1994).

3. MEASURING THE FRACTAL DIMENSION OF NATURAL OBJECTS

In this section, we summarize some of the more commonly used methods for estimating the fractal dimension D of natural objects. Formal mathematical derivations and proofs have been omitted; readers interested in fractal theory should consult Mandelbrot (1982), Voss (1988), Falconer (1990), Tricot (1991), or Hastings and Sugihara (1993). Note, however, that some of the methods used to estimate the fractal dimension are empirically, not mathematically, derived. Other reviews that have summarized fractal dimension estimation methods include Frontier (1987), Milne (1988, 1991a), Williamson and Lawton (1991), Kenkel and Walker (1993), Klinkenberg (1993), Nonnenmacher et al. (1994), Lorimer et al. (1994) and Johnson et al. (1995). Most of these reviews have been somewhat selective, or have focussed on a specific sub-discipline within the biological sciences. The diversity of available approaches for determining the fractal dimension reflects differences in objectives, and in the type of data analyzed.

3.1 Dividers (Compass) Method

This method is used to measure the fractal dimension of a curve (e.g. cell membrane, coastline, landscape edge). The procedure is analogous to moving a set of dividers of fixed length δ along the curve (**Fig. 2**). The estimated length of the coastline is the product of N (number of rulers required to 'cover' the object) and the scale factor δ. The power-law relationship between the measuring scale δ and the length L = Nδ is:

$$L = K\delta 1 - D \qquad \textbf{[3]}$$

The fractal dimension is estimated by measuring the length L of the curve at various scale values δ. Normant and Tricot (1991) note that this method is not well-founded theoretically, and furthermore is exact only for statistically self-similar curves (see also Tricot 1991). Because the value L = Nδ may vary depending on starting position along the curve, it is recommended that the procedure be repeated at different starting positions (Sugihara and May 1990). In some cases the log-log plot does not have a constant slope (i.e. the fractal dimension is not constant). While the point of slope change may indicate the operational scale of different generative processes (Kent and Wong 1982; Wiens 1989), it may simply reflect the limited spatial resolution of the data being analyzed (Hamilton et al. 1992; Kenkel and Walker 1993; Gautestad and Mysterud 1994).

Longley and Batty (1989) refer to the above procedure as the 'structured walk' method, and outline a number of variants of this basic procedure. Normant and Tricot (1991, 1993) have recently described an alternative estimation algorithm, termed the 'constant deviation variable step' (CDVS) method, that emphasizes the local behaviour of the curve. Their method is more complicated, as it involves division of the curve into a series of subarcs (local convex hulls) of given breadth ε. By varying ε, an estimate of the fractal dimension is obtained using a simple modification of the above

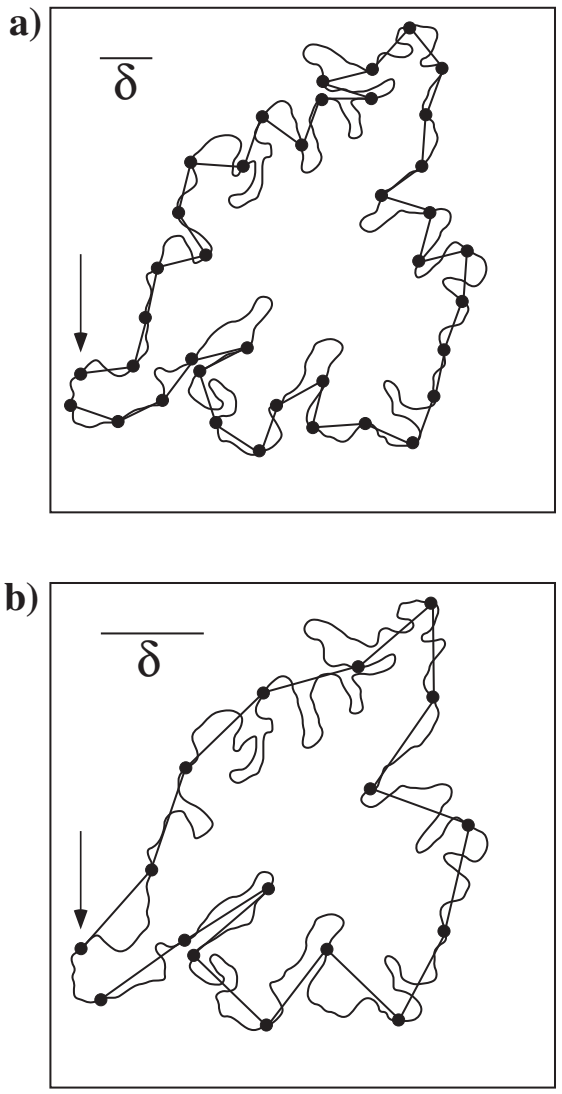

Fig. 2. Dividers (compass) method. Two ruler lengths (δ) are shown in (a) and (b). The starting position is indicated by an arrow.

equation. Tricot (1991) provides a detailed exposition on the analysis of nonrectifiable fractal curves. He is quite critical of empirical estimation methods, as evidenced by the following quote from the introduction to his book:

> "... it is quite surprising to find, even in the case of curves, how scarce, hazy, and unmathematical are our notions on the subject. The less precise our thoughts are, the fuzzier our practical scientific path will be. How many still think that the west coast of Great Britain is a self-similar curve, or that the 'compass method' allows us to estimate the fractal dimension ...?"

3.2 Grid (Box-Counting) Method

This procedure, like the dividers methods, can be used to measure the fractal dimension of a curve (Longley and Batty 1989). In addition, it can be applied to overlapping curves (Peitgen et al. 1992: 240) and structures lacking strict self-similar properties such as vegetation (Morse et al. 1985). Formally, the method finds the 'δ-cover' of the object, i.e. the number of pixels of length δ (or circles of radius δ) required to cover the object (Voss 1988: 60). A more practical alternative is to superimpose a regular grid of pixels of length δ on the object and count the number (C) of 'occupied' pixels (**Fig. 3**). This procedure is repeated using different values of δ. The defining power-law relationship is:

$$C = K\delta - D \qquad \textbf{[4]}$$

Because slight re-orientations of the grid can produce different values of C, grid placements should be randomly replicated to obtain a distribution of D-values (Appleby 1996). Tatsumi et al. (1989: 501) outline an analogous method for image-processing systems. Longley and Batty (1989) note that the box-counting method "may be less suited to the task of hugging the more intricate details of the base curve but, because of its low computer processing requirements, it is recommended

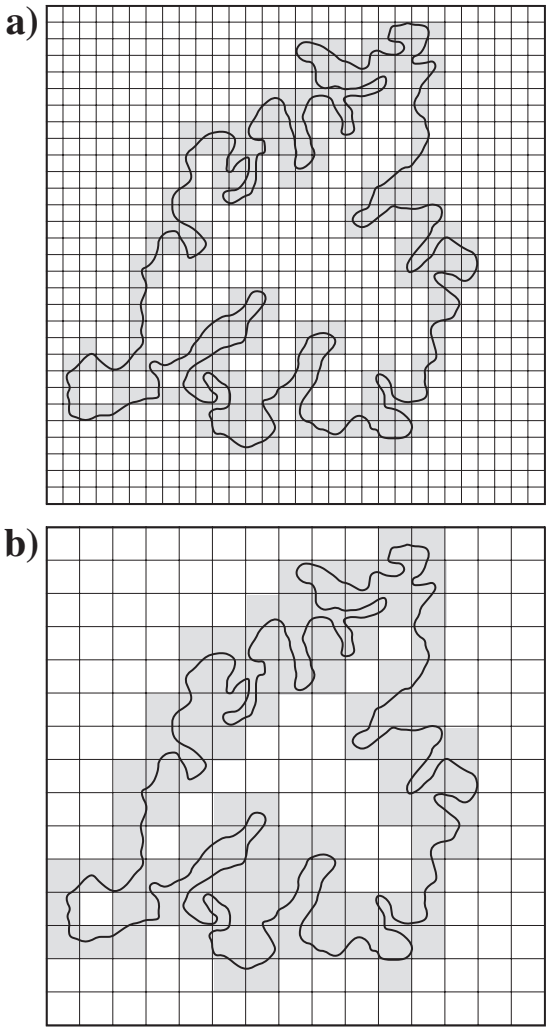

Fig. 3. Grid method: border or line image. Two box 'lengths' are shown in (a) and (b). Boxes including the image are shaded.

as a method suitable for yielding a first approximation to the fractal dimension". Normant and Tricot (1991) are more critical, stating that the box-counting method is "often unusable and, in any case, yields very imprecise results". Pruess (1995) demonstrates that the limited resolution of most data renders the estimation of D sensitive to the range of box lengths δ used.

Morse et al. (1985) describe a box-counting method for estimating the fractal dimension of ecological habitats ($2 \leq D \leq 3$). Consider the problem of estimating the fractal dimension of a tree branch. In principal, a three-dimensional grid system could be superimposed on the branch and the size of 'counting-cubes' varied. Such a procedure is impossible to implement in the field, however, at least given present technical limitations (Zeide and Gresham 1991: 1209). Morse et al. (1985) simplified the problem by obtaining a two-dimensional photographic image of the habitat, the fractal dimension of which was determined using the box-counting method ($1 \leq D \leq 2$). Following Mandelbrot (1982: 365), they determined heuristic lower (D+1) and upper (2D) limits of the 'habitat' fractal dimension under the assumption that the photograph is a randomly-placed orthogonal plane. The resulting limits are rather broad (e.g. if D = 1.3, the limits are 2.3 - 2.6). Despite this limitation, and evidence suggesting that extrapolation to higher dimensions is invalid (Roy et al. 1987; Huang and Turcotte 1989), the procedure has since been used by others to estimate habitat fractal dimensions (e.g. Shorrocks et al. 1991; Gunnarsson 1993). Cube-counting methods can be used to estimate D of coded surfaces (Milne 1988: 73) and animal territories (Milne 1991a).

The box-counting method can also been used to determine the fractal dimension of pixel images (Milne 1992: 44; Virkkala 1993). Consider a map in which states of interest are coded either 'on' (1) or 'off' (0). To determine the fractal dimension of the 'on' pixels, divide the image into coarser scales of pixel resolution ('windows') and count the number of windows occupied by a least one 'on' pixel (**Fig. 4**). The log-log plot (resolution scale vs. number of windows occupied) is used to determine the fractal dimension (D = -slope). De Cola (1991) describes a related method, based on hierarchical grouping of adjacent pixels, for determining the fractal dimension of spatial autocorrelation. Virkkala (1993) used a similar method to determine the fractal dimension of passerine birds distributions in central Finland. Gautestad and Mysterud (1994) note that Virkkala's (1993) approach is incorrect. They offer

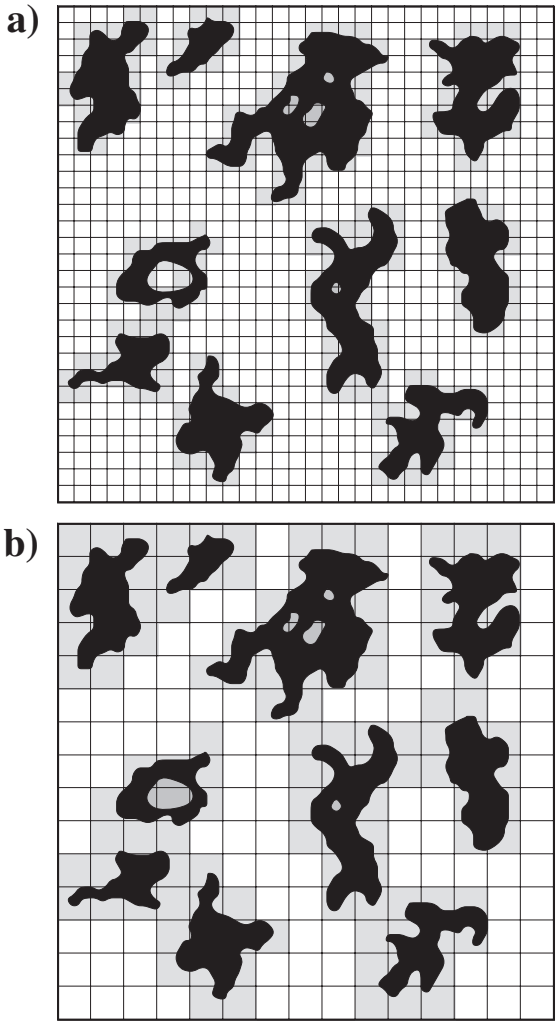

Fig. 4. Grid method: pixel or filled image (solid black). Two box 'lengths' are shown in (a) and (b). Boxes including the image are shaded.

a correction, but note that the limited resolution of most distributional data (the so-called 'dilution effect') can severely bias fractal dimension estimates.

Taylor and Taylor (1991) point out that the limited resolution of digitized images results in an underestimation of counts for smaller boxes, resulting in a convex log-log plot (and an underestimate of D). They propose an image filtering algorithm in which cells that are 'off' in the original image are selectively turned 'on'. The idea is that, for (say) a 3 x 3 window in which only the central cell is 'on', there is a finite probability that some or all of the adjacent eight cells should also be included in the box count. Probabilities are assigned to the cells using a binomial model and solving for p:

$$3D - 1 = 8\,pB \qquad \textbf{[5]}$$

where D is the box dimension of the original (uncorrected) image and B is the observed mean number of 'on' neighbours (for a more complete description see

Taylor and Taylor 1991: 358). Cells with probability values exceeding a specified threshold are switched 'on' and the box-dimension recalculated.

3.3 Area-Perimeter Relationships

Area-perimeter methods are generally used to estimate the fractal dimension of objects ('islands') coded as raster-based digitized images. Depending on objectives, three approaches are possible: (a) perimeter-based, to determine the extent that an island perimeter fills the plane; (b) area-based, to determine the extent that the island itself fills the plane; (c) landscape-based (islands divided into different types), to compare island complexity. These methods can be used to determine the 'mean' fractal dimension of a set of islands, or to determine D for each island. The method used will depend on the objectives of the study. As an example, consider a landscape consisting of pixel 'islands' (**Fig. 5a**). A study focussing on ecotonal boundaries (edges) would use the perimeter dimension method. With this method, convoluted islands have a high D, as do long and thin islands. A study focussing on acquisition and retention of space, however, would use the area dimension. This method computes a high fractal dimension for objects that best 'fill up' two-dimensional space (i.e. isodiametric islands). Here, the argument can be made that an isodiametric patch of vegetation (area to edge ratio high) is more likely to retain that space than a thin, convoluted patch (area to edge ratio low). Both methods measure a fractal dimension, but application and interpretation are quite different.

Perimeter Dimension

This method measures the extent that patch perimeters 'fill' the two-dimensional plane. The perimeter-area relationship for a set of islands is given by:

$$P = kA^{D/2} \qquad \textbf{[6]}$$

where the area A is the number of pixels making up a given object, the perimeter P is a count of the number of pixel edges, and k is a scaling constant. The slope of the log-log area-perimeter plot for a set of objects gives a 'mean' fractal dimension (Burrough 1986:127). Landscapes with perfectly square objects (perimeter: area ratio low) have a fractal dimension D = 1, while those containing highly complex convoluted objects (perimeter:area ratio high) have fractal dimensions approaching 2. In effect, the method determines the relative 'edginess' of an image. For a single island, the perimeter dimension reduces to D = 2 log(P)/log(A).

A digital image of a fractal object is Euclidean by virtue of its being placed onto a grid, leading to biased estimates of D. To account for this 'rectangularization', the perimeter P is expressed as P/4, where the value 4 is determined as the proportionality constant for a pixel system. The limitations of a square grid means that the maximum value for D = 2 (A - 1), where A is the island area. The island perimeter should therefore be measured

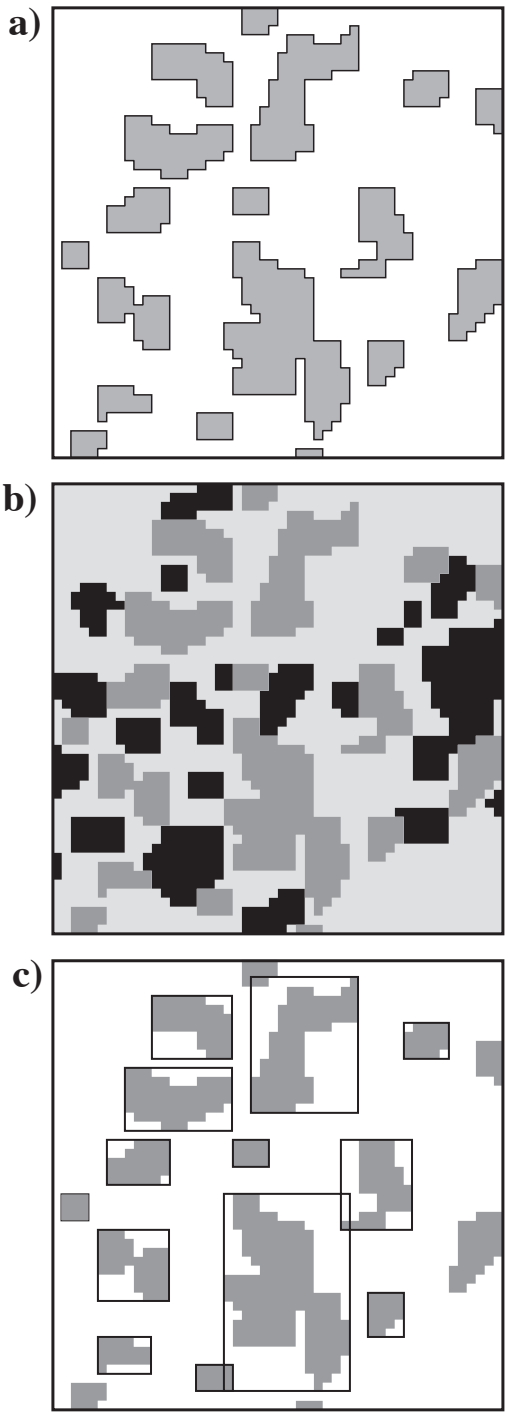

Fig 5. Area-perimeter relationships. (a) Landscape of pixel 'islands'. The area of each island in shaded, and its perimeter is indicated by a solid black line; (b) Determination of L (row and column lengths of pixel-islands) for computation of the box dimension; (c) Landscape of three island types, indicated by different shading levels.

using the expression [P + (2 (A - 1))]/4 when estimating D using the perimeter-area method (Olsen et al. 1993). Milne (1991a: 224-226) notes that rectangularization is particularly problematic when islands are small (A < 30). Edge effects are also a problem: inclusion of 'islands' abutting the edge of the study area will result in a biased estimate of the fractal dimension. The simplest solution is to ignore these islands, but this will tend to exclude larger, more convoluted islands and so bias the D estimate. A final problem relates to the representation of digital images. A line drawn at 45° to the horizontal is approximated as a 'staircase' of pixels, resulting in a considerable increase in the 'perimeter' of an object relative to its area. In preliminary studies, we found that estimates of D depended on the orientation of an image during scanning. We recommend that the image be digitized in a number of orientations to quantify this variation.

Area Dimension

This method quantifies the proportion of the plane that is occupied by an island. Voss (1988: 61) suggests that the 'box' dimension of an island can be measured as D = log A/log L, where L is the maximum of the row and column lengths of the pixel-island (**Fig. 5b**). Square islands (A = n2, L = n) completely fill the two-dimensional space (D = log n2/log n = 2), while for rectangular islands of length n and width 1 (A = n x 1, L = n), D = log n/log n = 1. Milne (1991a: 225) suggests as an alternative the 'area' dimension D = log A/log (P/4). Unfortunately, the relationship between these two area-perimeter measures (and to the perimeter dimension) are poorly understood. If an archipelago of islands is characterized using this method, the determining length-area relationship is:

$$A = LD \qquad \textbf{[7]}$$

Landscape dimension

For an image composed of several island types (e.g. habitat classification map, **Fig. 5c**), a measure of D that considers island adjacency is desirable. Specifically, the extent to which the perimeter of a given island type interacts with neighbouring island types is incorporated into the measure of fractal dimension. Olsen et al. (1993) calculate a modified perimeter length:

$$P_m = P + \left[2(A-1)\left(C/(C_t - 1)\right)\right] \qquad \textbf{[8]}$$

where P and A are the island perimeter and area respectively, C is the count of the number of adjacent island types, and C_t is the total count of all island types in the image. A modified fractal dimension is then calculated for the landscape by substituting the new perimeter measure into the perimeter-area power law relation:

$$D_m = 2\left[\ln(P_m/4)/\ln(A)\right] \qquad \textbf{[9]}$$

3.4 Probability-Density Function

This method was originally developed to analyze point pattern data (Voss 1988), but has most commonly been used to estimate the fractal dimension of a raster image (e.g. Milne 1992). Unlike the perimeter-area methods, discrete habitat islands are not required. The probability-density function ϱL is obtained from square (L x L) sampling 'windows' successively placed over each 'on' pixel (**Fig. 6a**). Within each window, a count is made of the number (n) of 'on' pixels. Count frequencies are then expressed as probabilities (**Fig. 6b,c**):

$$\sum_{n=1}^{N(L)} \rho L = 1 \qquad \textbf{[10]}$$

where N(L) ≤ L2. For a given value of L, the first moment of the probability distribution is given by:

$$M(L) = \sum_{n=1}^{N(L)} n\rho L \qquad \textbf{[11]}$$

which is termed the 'mass dimension'. These computations are repeated for various values of L. Because each window is centred on a single pixel, L must be an odd number. Voss (1988: 66-67) shows that the following power law holds for fractal images:

$$M(L) = kLD \qquad \textbf{[12]}$$

Thus the fractal dimension D can be estimated from the log-log plot of the first moment as a function of L (Milne 1991b). Note that higher-order moments of the function can also be defined (see **Section 4**).

Milne (1992: 41-45) compared three artificial landscapes (each half-covered with 'filled' pixels) to determine the behaviour of this method. The method can also be used to estimate the dimension of fractal surfaces, though it gives poor estimates for surfaces of D > 2.5. To overcome this problem, Keller et al. (1989) suggest a linear interpolation correction. Note that increases in the window size (L) result in exclusion of a greater proportion of pixels along the periphery of the map. Under assumptions of isotropy, a toroidal edge correction can be used to circumvent this problem.

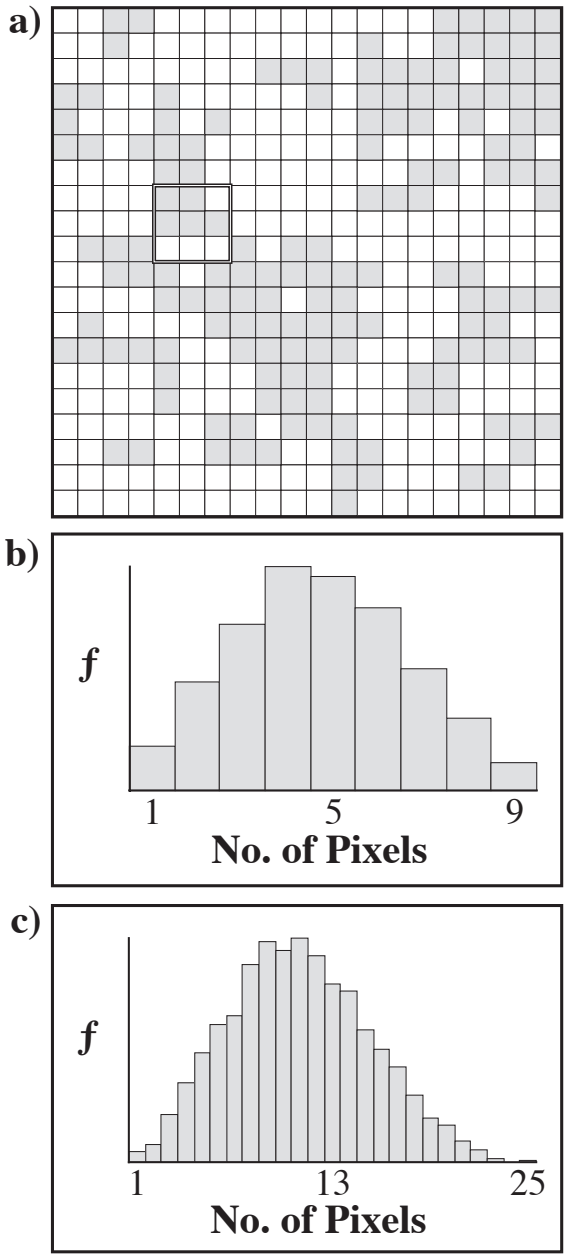

Fig. 6. Probability-density function. (a) Pixel map (shaded regions), showing a representative 3x3 sliding window (double line) for which the count = 5; (b) Frequency distribution of pixel counts for a 3x3 window; (c) Frequency distribution of pixel counts for a 5x5 window.

3.5 Size-Frequency Distributions

Distribution of Areas (Korcak Empirical Relation)

For an archipelago of 'self-similar' islands, the relationship between island size (area) and frequency is given by the cumulative hypergeometric size-frequency distribution (Burrough 1986:127):

$$N = ka\left(-D/2\right) \qquad \textbf{[13]}$$

where N is the number of islands larger than area a. (**Fig. 7**). This function implies that an archipelago of irregularly-shaped islands (i.e. D large) will be dominated by many small islands.

Hastings et al. (1982), following Mandelbrot (1982), suggested that there is a relationship between persistence (H = Hurst (1951) parameter of the fractional Brownian motion (fBm) model; Peters 1994: 53) and landscape fragmentation (D = fractal dimension of patches as determined from the hypergeometric distribution). While the exact relationship between D and H depends on the model chosen, Sugihara and May (1990) state that "increased persistence (more memory in the process) should correspond to smoother boundaries and patches with larger and more uniform areas; whereas reduced persistence will correspond to more complex and highly fragmented landscapes dominated by many small areas". Under certain limiting assumptions (Sugihara and May 1990: 83), the relationship between H and D is:

$$H = 2 - D \qquad \textbf{[14]}$$

This implies that landscapes with many small islands show greater boundary complex (high D) and are less persistent (low H). Sugihara and May (1990: 83) summarize the relationship as:

H	*D*	*Correlation*	*Nature of Process*
> 0.5	< 1.5	positive	'persistent'
$= 0.5$	$= 1.5$	zero	Brownian (random)
< 0.5	> 1.5	negative	'anti-persistent'

Persistence refers to the degree of autocorrelation of adjacencies: for $H < 0.5$, a fractional Brownian motion trace is negatively correlated, whereas values are positively correlated for $H > 0.5$. Hastings et al. (1982) used this method to compare cypress (early successional) and broadleaf evergreen (late successional) patches in Okefenokee Swamp. They found that cypress patches had a higher fractal dimension (D = 1.25, H = 0.75) than broadleaf evergreen patches (D =1.0, H = 1.0), implying that the earlier successional vegetation shows greater patchiness and decreased persistence (see also Hastings and Sugihara 1993:126). A later study (Meltzer and Hastings 1992) points out a number of methodological problems associated with the approach. While the method may prove useful in remote sensing (Sugihara and May 1990), objective tests are required to determine whether persistence-patchiness relationships developed under limiting theoretical assumptions are valid for ecological systems (Johnson et al. 1995).

In a study of lake geometry in tropical river flood

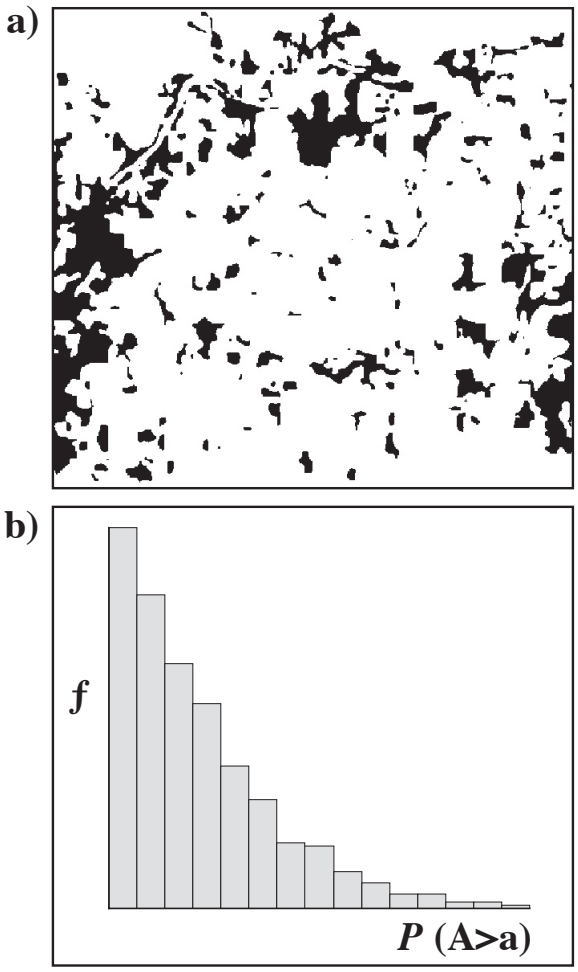

Fig. 7. Size-frequency distributions. (a) Map of forest patches on public land between Riding Mountain National Park and Duck Mountain Provincial Forest, Manitoba; (b) Cumulative size-frequency distribution for the image in (a).

basins, Hamilton et al. (1992) found that fractal dimensions calculated were "infeasible", with some values approaching 3. They attributed this to censorship and truncation. Censorship occurs as lake sizes approach the spatial resolution of the image (attributable to satellite limitations, or possibly the seasonality of smaller lakes). Truncation reflects the physical impossibility of having lakes larger than the area of the floodbasin. Violations of the isodiametry assumption can also inflate estimates of the fractal dimension. Walker (unpublished data) found that high D-values for habitat patches in Riding Mountain National Park, Canada reflected the linearity of drainage patterns in the region.

Distribution of Volumes (Rosin's Law)

Turcotte (1986) described the hypergeometric frequency distribution relation (Rosin's Law) for particle size in soils and other geological material as:

$$N = kR_i - D \qquad \textbf{[15]}$$

where N is the number of particles whose radius is greater than Ri, and D is the fractal dimension. Perfect et al. (1992) derived a version of Rosin's Law for use with soil mass data. A higher fractal dimension indicates greater soil fragmentation and a soil increasingly dominated by small particles (Tyler and Wheatcraft 1989):

Fractal Dimension	***Nature of Soil***
D = 0	all particles are of equal diameter.
D = 3	number of particles greater than a given radius Ri doubles with each corresponding decrease in particle mass.
0 < D < 3	greater proportion of larger particles than D = 3 (sand).
D > 3	greater proportion of smaller particles than D = 3 (silt, clay).

Tyler and Wheatcraft (1989) show that silt-clay soils have fractal dimensions in the range 3.0-3.5. They computed one-dimensional 'pore trace' D values for soils using a method suggested by Mandelbrot et al. (1984). For a soil of fractal dimension D = 3.2, the fractal increment Di = D - 3 = 0.2 measures the degree to which the soil 'exceeds' the Euclidean three-dimensional space. The one-dimensional pore trace is simply 1 + Di = 1.2. A trace of D = 2 would completely fill the space, as expected for a soil containing a high proportion of very fine particles.

Rieu and Sposito (1991a) developed a soil porosity model under the assumption that soil is a fragmented, fractal porous medium. Using this model, soil water potential was shown to be a function of fractal dimension:

$$h_i = h_o\left[(1-\phi)+\theta_i\right]1/(Dr-3) \qquad \textbf{[16]}$$

where hi = soil water potential, ϕ = soil porosity, θi = volumetric water content, and Dr is the 'bulk fractal dimension'. Rieu and Sposito (1991b) found good agreement between Dr and the D determined using Rosin's law.

3.6 Branch Order Relationships

The relationship between mean bronchial tube diameter and branch order was examined by West and Goldberger (1987). The defining power-law relationship is:

$$R(z) = A(z)/zD \qquad \textbf{[17]}$$

where R(z) is the mean tube diameter at the z^{th} gen-

eration, A(z) is a constant periodic function, and D is the fractal dimension. This fractal model predicts that decreases in mean tube diameter with each generation follow a power-law relationship. For bronchial tube length, the relationship is:

$$L(z) = A(z)/z1 - D \quad \textbf{[18]}$$

where L(z) is the mean tube length at the zth generation (**Fig. 8**). Using this relation, Crawford and Young (1990) found that branching pattern of two species of oak is consistent with a power-law model.

3.7 Spatial and Temporal Series

These methods are used to examine the fractal properties of a spatial or temporal series. For a temporal series, the fractal dimension describes the relationship between signal variance and time scale (Schepers et al. 1992).

Semivariance

The semivariance γh of a spatial or temporal series (Curran 1988):

$$\gamma_h = 1/(2N_h)\sum_{i=1}^{N_h}(X_i - X_{i+h})^2 \quad \textbf{[19]}$$

is the variance at lag interval h. The semivariogram plot (γh as a function of h) reaches a maximum (the so-called 'sill') at a lag distance L (**Fig. 9**). The sill semivariance γL approximately equals the variance of the data, while distance L specifies the range of spatial or temporal dependence (Phillips 1985). It can be shown (Burrough 1983) that the fractal dimension of the series is described by:

$$2\gamma_h = h\beta \quad \textbf{[20]}$$

where β = 4-2D. The log-log semivariogram is used to determine the fractal dimension (Burrough 1986:127), where β is the slope of the linear portion of a semivariogram (h < L). For white noise, β=0 and the fractal dimension D = 2. Conversely, for a simple linear trend (spatial dependence at all scales) β=2, giving D = 1. For a statistically self-similar series, D = 1.5 (Palmer 1988: 94).

Burrough (1981) used semivariance to determine the fractal dimension of landscapes and environmental data. Fractal dimensions were generally quite high: for example, D = 1.5 for successive values of soil pH. Soil sodium levels had a fractal dimension D = 1.9, meaning that successive values in the sequence are nearly independent. Palmer (1988) used the semivariance method to examine spatial dependence of vegetation along transects, and Taylor (1988) used a related approach to determine the fractal geometry of tree ring increments.

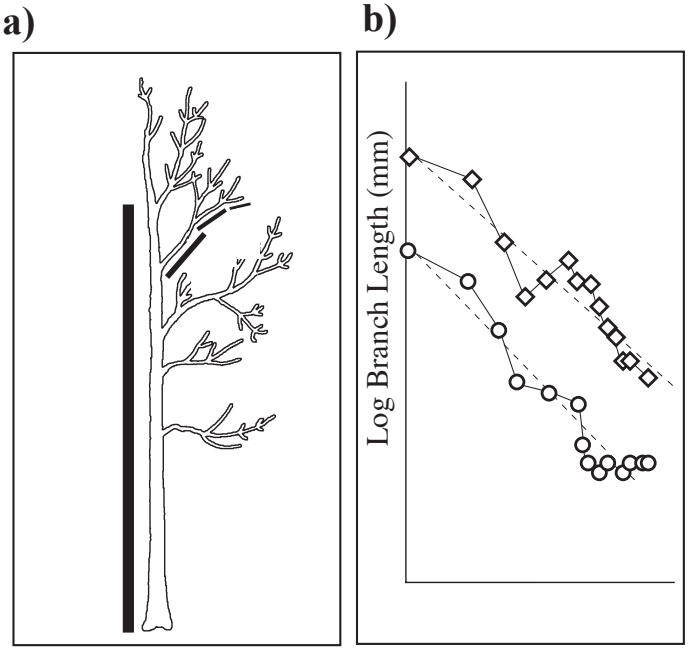

Fig. 8. Branch order relationships. (a) Branch order for a tree; (b) Example of branch order relationships in two species (diamonds and circles). Slopes of the log-log plots are indicated by dashed lines.

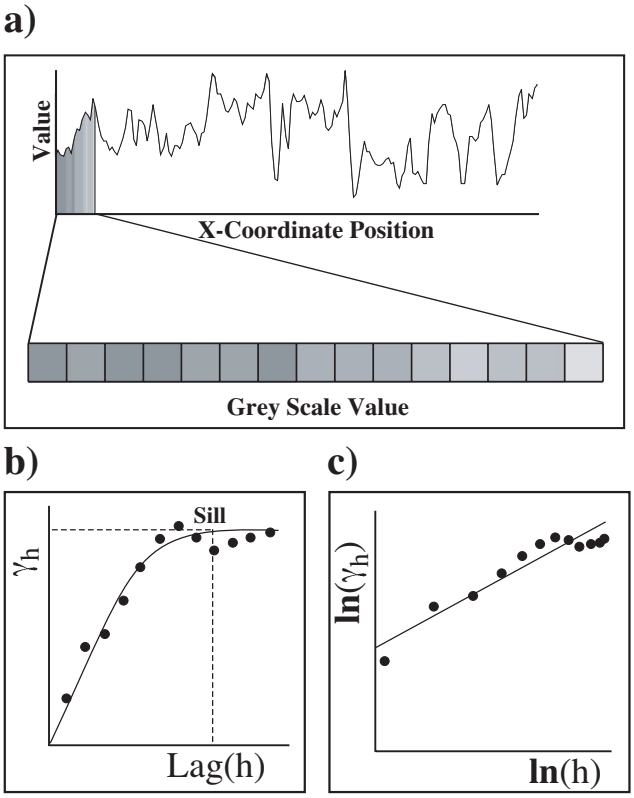

Fig. 9. Spatial and temporal series: semivariance. (a) Successive values as a function of distance (coordinate position); (b) Semivariance plot, showing the sill value; (c) Log-log plot of semivariance as a function of lag distance (for values below the sill). The fitted line is used to estimate D.

Russell et al. (1992) determined D for the distribution of a marine predator (auklet) and its prey (a species of copepod) along ocean transects off the Alaskan coast. They found that values of D for predator and prey were similar, which suggests that the foraging patterns of auklets match the multiscale complexity of their food resource.

Curran (1988) found that the 'ideal' semivariogram form (i.e. a distinct range and defined sill) is often not found in remotely sensed data. He noted that the 'grain' size (e.g. 30x30 m pixels in Landsat imagery) may exceed the range over which a particular variable is spatially dependent. Leduc et al. (1994) examined the robustness of semivariance in estimating the fractal dimension of landscapes. They found that landscapes are rarely self-similar over all spatial scales, and that they often display anisotropy. It was also found that grain size can affect the estimate of D.

Spectral Analysis

Spectral analysis has been used extensively in medicine (e.g. Liebovitch et al. 1987; Goldberger et al. 1990) and geology (e.g. Huang and Turcotte 1989) to estimate D of temporal and spatial series. The power spectrum is defined as the square of the amplitude A of a Fourier transform. The spectral behaviour for pure fractional Brownian motion (fBm) is given by:

$$P(\omega) = \left[|\omega|^{\beta}\right] - 1 \qquad \textbf{[21]}$$

where P(ω) is the power spectrum, |ω| is the spectral frequency, β = 2H+1, and H=2-D is the Hurst coefficient (Fortin et al. 1992). Because of the difficulty of estimating H directly from the fBm, the first differences of the signal (known as fractional Brownian noise, fBn) are normally used instead (**Fig. 10**). The spectral behaviour of fBn is as above, except that β = 2H-1. If successive fBn increments are completely uncorrelated, H= 0.5 and D= 1.5. For fractal dimensions D < 1.5 (H > 0.5), successive increments in the series are positively correlated. Correlations are higher and extend longer (i.e. the series has greater 'memory' or 'persistence' over time) as H increases. For D > 1.5 (H < 0.5), successive increments are negatively correlated.

A number of other methods for estimating the fractal dimension of time series have been described. Schepers et al. (1992), in a comparison of four methods, found that spectral analysis gave the most precise and accurate results. The other three methods tested (relative dispersion, correlation, and Hurst's rescaled range analysis) gave highly biased results and are not described here (see Hastings and Sugihara 1993: 56-59). A crude, empirical measure of waveform fractal dimension derived by Katz (1988) is also not recommended (Kenkel and Walker 1993).

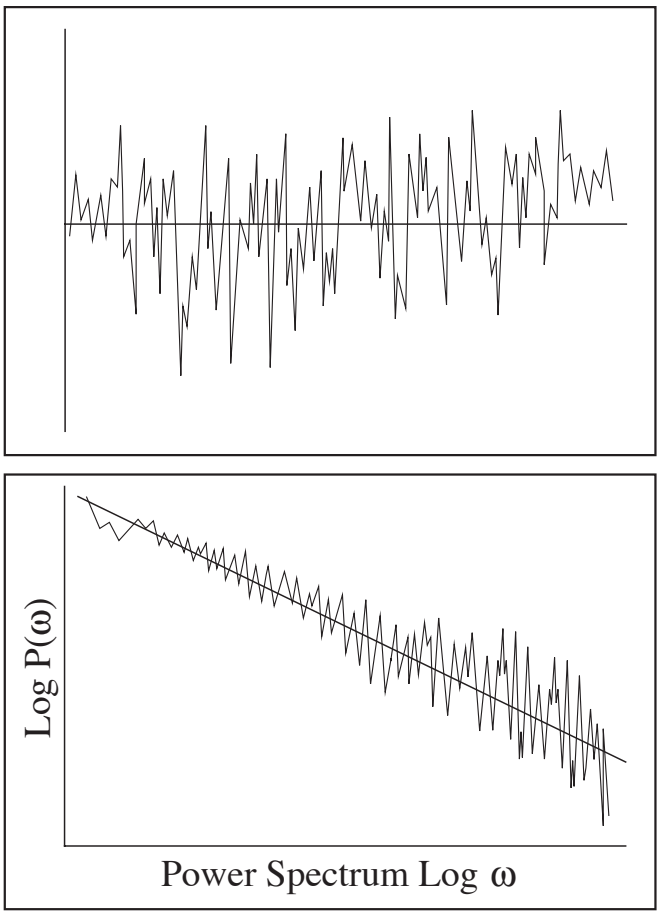

Fig. 10. Spatial and temporal series: spectral analysis. (a) First differences of a signal; (b) Power spectrum plot (log ω vs. log P(ω)) for the signal spectrum in (a). The fitted line is used to estimate D.

3.8 Point Patterns

These methods are used to determine the extent of self-similar spatial clustering in point patterns (**Fig. 11a)**. Statistically self-similar spatial point patterns can be generated using the Lévy dust model (Mandelbrot 1982: § 32). The more highly clustered the points (at all spatial scales), the lower the fractal dimension.

Palm Intensity

For a set of coordinates of points on the plane $[\rho_1, \rho_2, ..., \rho_n]$, compute all pairwise vector 'distances':

$$\Delta_{i,j} = \left|\rho_i - \rho_j\right| \quad (i = 1 \text{ to } n;\ j = 1 \text{ to } n;\ i \neq j) \qquad \textbf{[22]}$$

A nonparametric estimation of the Palm intensity is found by counting the number of vectors within an

annular region of area A (with radii of u1 and u2). Dividing this value by A gives an estimate of the Palm intensity $\lambda(\Delta)$ at $\Delta = u$ (where $u1 \leq u < u2$). The log-log plot of $\lambda(\Delta)$ vs. u has slope $H = 2 - D$ under certain limiting conditions. A parametric maximum likelihood estimation method for D is derived by Ogata and Katsura (1991: 465-466). This method requires a large number of points (>1000) to obtain a reasonable estimate of D.

Spectral Intensity

This method is related to the power spectrum procedure outlined above. The averaged marginal periodogram with respect to wave number (ω_r) is estimated as:

$$\Delta(\omega_r) = J - 1\sum_{j=1}^{J} I\left(\omega_r \cos\omega\theta_j, \omega r \sin\omega\theta_j\right) \quad \textbf{[23]}$$

The linear portion of the log-log plot of $\Delta(\omega_r)$ vs. ω_r has slope = -D. However, Ogata and Katsura (1991: 467) recommend that D be determined using parametric maximum likelihood estimation.

Grid (Box-Counting) Method

The box-counting method described previously can be applied to two-dimensional point patterns to estimate the 'cluster' dimension (Hastings and Sugihara 1993:44), with range $1 \leq D \leq 2$ (**Fig. 11b,c**). The cluster dimension can also be computed using 'counting-disks' instead of boxes (Frontier 1987:350). Robertson and Sammis (1995) outline a cube-counting version for use with three-dimensional point patterns. They discuss some problems with cube-counting methods and offer strategies for resolving these problems.

King et al. (1989) suggest counting the number of points within each grid unit of size δ and determining the relative dispersion (RD) = (standard deviation)/(mean) of grid counts. Repeating this for various values of δ defines a power law relationship between number of pixels and relative dispersion:

$$RD = KnD - 1 \quad \textbf{[24]}$$

Random uncorrelated noise has a fractal dimension D = 1.5, while a value of D = 1.0 reflects "uniformity of the property over all length scales" (King et al. 1989). The spatial correlation between regions of defined size or separation distance is given by:

$$r = 23 - 2D - 1 \quad \textbf{[25]}$$

For D = 1.5 (random pattern), the correlation r = 0, while for D = 1.0 the correlation is maximal (r = 1.0).

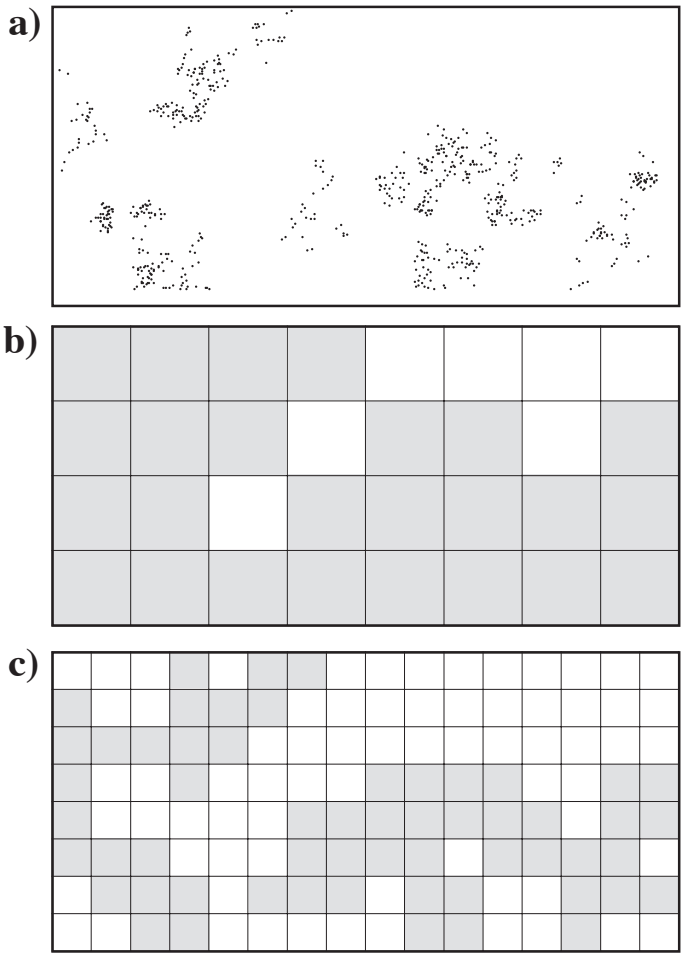

Fig. 11. Point pattern analysis: box-counting method. (a) A self-similar point pattern, generated using the Lévy flight model; (b,c) Shaded boxes are occupied by at least one point.

Cumulative Distance Method

Hastings et al. (1992) suggested a power law relationship for the cumulative number of points N(r) within a distance r:

$$N(r) = krD \quad \textbf{[26]}$$

This relationship assumes a Poisson distribution within a D-dimensional space (Hastings and Sugihara (1993: 45). Using this method, Hastings et al. (1992) demonstrated that the distribution of pancreatic islets in planar sections had a fractal dimension D = 1.55. This implies that increasing the area four-fold will result in 21.55 = 2.93 additional islet points, not 22 = 4 as would be expected if the pattern were statistically random (D = 2).

3.9 Information Theory and Diversity

Consider again a square grid (box size δ) superimposed on an observed point pattern. Within each occupied grid unit, the number of points ni is counted (**Fig. 12**). Each count is then expressed as a proportional

a)

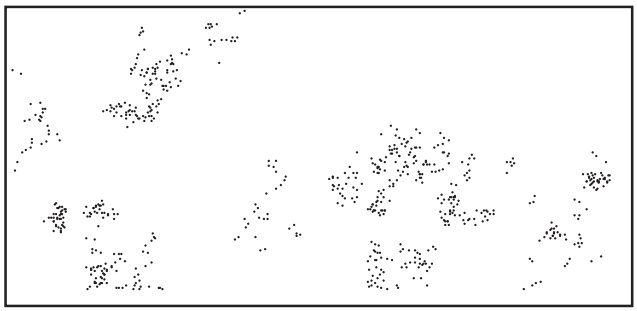

b)

2	26	32	1				
17	55	8		11	28		2
37	30		22	74	78	24	44
2	70	2	6	31	29	12	19

c)

			4		14	1									
2			22	16	2										
7	1	13	38	8											
9			4					1	10	19	9			1	1
2						7	3	21	25	26	16	6		13	23
1	34	30				10	2	7	21		36	12	6	8	
	2	20	10		2	3	3		16	25			8	18	1
		26	14						15	4			4		

Fig. 12. Point pattern analysis: information and correlation dimension. (a) A self-similar point pattern, as in Fig. 11; (b,c) Number of points per box at two box 'lengths'.

value:

$$p_i = n_i / N \qquad \textbf{[27]}$$

where N is the total number of points in the set. Milne (1988: 71-75) considers scaling relationships in the context of the Shannon entropy:

$$H\delta = \sum_{i=1}^{N\delta} p_i \log p_i \qquad \textbf{[28]}$$

where Nδ is the number of occupied boxes (e.g. quadrats) of size δ. For fractal processes, H scales as:

$$H\delta = Ho - \sigma \log \delta \qquad \textbf{[29]}$$

where Ho is a constant (H as δ approaches 0), and σ is the 'information dimension' (the lower bound of the Hausdorf dimension, Grassberger and Procaccia 1983; Scheuring and Riedi 1994). The information dimension is thus obtained as the slope of the Hδ vs. δ plot.

Farmer et al. (1983) discuss the relationship between the fractal dimension D and the information dimension σ. They point out that D is a 'metric dimension' (i.e. depending on metric scaling properties), whereas σ is a 'probabilistic dimension' (i.e. depending on both metric and probabilistic properties). Under some circumstances D = σ, although in general D > σ. The information dimension is sometimes referred to as the 'dimension of the natural measure' (Farmer et al. 1983; Loehle and Wein 1994).

Frontier (1987: 358-364) demonstrates that the familiar Shannon evenness measure J = H/Hmax can be thought of as a measure of the fractal dimension of the distribution of individuals among species (see also Johnson et al. 1995).

For fractal sets, the Simpson diversity index:

$$C\delta = \sum_{i=1}^{N\delta} p_i^{\,2} \qquad \textbf{[30]}$$

scales as:

$$C\delta = K\delta D \qquad \textbf{[31]}$$

where D is the so-called 'correlation dimension' (Henctschel and Procaccia 1983). In practice, D determined as the slope of the log Cδ vs. log δ plot (Wallinga 1995).

3.10 Surface Models

Polidori et al. (1991) derive a straightforward algorithm for direct estimation of the fractal dimension of topographic surfaces (**Fig. 13a**). Their method is derived from the fractional Brownian motion model described in **Section 3.5** (see also Goodchild 1980; Sugihara and May 1990: 83). An estimate of the fractal dimension ($2 \le D \le 3$) is obtained from the relation:

$$\log|e| = \log k + H \log d \qquad \textbf{[32]}$$

where |e| is the mean absolute elevation (height) difference between points that are a horizontal Euclidean distance d apart. A measure of fractal dimension is given by D = 3 - H. Polidori et al. (1991) interpret the Brownian parameter H as follows:

H	*D*	*Interpretation*
> 0.5	< 2.5	height variations likely have the same sign.
$= 0.5$	$= 2.5$	height variations are independent.
< 0.5	> 2.5	height variations likely have opposite signs.

As expected, the fractal dimension of 'rough' topographic surfaces (negative correlation of height varia-

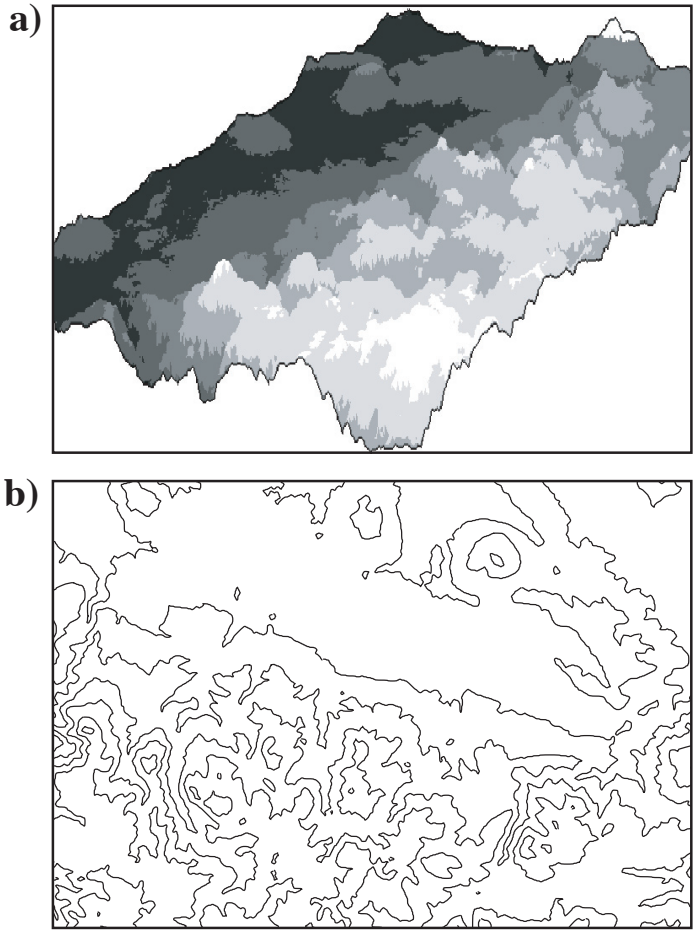

Fig. 13. Surface models. (a) Example of a three-dimensional topographic surface, with higher elevations represented by lighter shades of grey; (b) Contour map of the surface shown in (a).

tion) is high, while smooth surfaces (positive correlation of height variation with distance) have a low fractal dimension.

The semivariance and spectral methods outlined above are easily modified to determine the fractal dimension of landscape surfaces (Huang and Turcotte 1989). For the semivariance:

$$\gamma_h = \frac{1}{(4N_h)} \sum_{i=1}^{N_h} \sum_{j=1}^{N_h} \left[\left(X_{ij} - X_{i+h,j} \right)^2 + \left(X_{ij} - X_{i,j+h} \right)^2 \right] \quad \textbf{[33]}$$

From the log-log semivariogram, D = 3 - slope/2 (Bian and Walsh 1993).

Surface fractal dimension can also be estimated indirectly by examining 'profiles' (one-dimensional transects) taken from the surface. Lam (1990; see also Goodchild 1980) used a cell-counting algorithm based on the fractional Brownian motion model. At various step sizes, counts are made along 'profiles'. The fractal dimension is estimated separately for each profile from the log-log plot of cell count against step size (D = 2 - slope, where $1 \leq D \leq 2$). The average of these values plus one provides an estimate of the surface fractal dimension. Another method involves 'converting' the surface plot to a contour map (Fig. 13b), and using the dividers method to determine the fractal dimension of the contours (the surface fractal dimension is equal to the mean of these D-values plus one). Roy et al. (1987) compared some of these methods and found that they can give quite different results (e.g. D ranged between 2.01 - 2.33 for the same image). Their study also found that the fractal dimension of many images varies spatially.

3.11 Two-Surface Method

Zeide and Pfeifer (1991; also Zeide and Gresham 1991) developed an empirical procedure for estimating the fractal dimension of tree crowns. They point out that it is currently impossible to estimate tree crown D using the 'cube-counting' method. As an alternative, they suggest a power law relating two easily obtained measures, total leaf area and the surface area of a convex hull enveloping the tree crown. If leaf area and crown surface area are equal, it can be inferred that leaves are largely restricted to the surface of the crown (as in shade-tolerant tree species growing in the understory). The tree crown therefore has a 'planar' form with fractal dimension D = 2. An increase in leaf area implies that more leaves occur inside the crown, which increases the fractal dimension of the canopy. The defining relation is:

$$A = kED/2 \quad \textbf{[34]}$$

where A is the total leaf area and E is an estimate of the surface area of a convex hull that envelops the crown. As this is a measure of crown surface, $2 \leq D \leq 3$. Zeide and Gresham (1991) suggest that crown fractal dimension may vary with site quality and thinning intensity, and therefore may be a useful indicator of site conditions. Zeide (1991) and Lorimer et al. (1994) discuss additional applications of fractal geometry to forestry.

4. MULTIFRACTALS

Thus far, it has been emphasized that a single scaling exponent D characterizes a fractal object or structure. However, many natural fractal-like structures are determined by a large number of generating processes operating at different scales (Loehle and Wein 1994; Scheuring and Riedi 1994). Such structures (termed multifractals) are characterized by fractional dimensions that vary in scale, and so require an infinite number (distributional spectrum) of scaling exponents for

their description (Stanley & Meakin 1988). Appleby (1996) outlines a straightforward iterative algorithm for generating multifractal point patterns.

As an introduction to multifractals, consider again a spatial pattern of N points (Fig. 12a). A grid of boxes of length δ is laid over the pattern, and a count of the number of points in each of the Nδ occupied grid boxes is determined (Fig. 12b,c). Express each box count as a proportion:

$$p_i = n_i / N \qquad \textbf{[35]}$$

The generalized entropy (Rényi 1970) is defined as:

$$Iq(\delta) = 1/(1-q)\log\sum_{i=1}^{N\delta} p_i q \qquad \textbf{[36]}$$

By varying q, an entire family of entropy functions is defined:

q	*Iq(δ)*	*Name*	*Dimension*
0	log Nδ	log(box count)	box-count
⇒1	-Σ p_i log p_i	Shannon entropy	information
2	- log Σ p_i^2	log(Simpson index)	correlation

The generalized dimension D_q for the q^{th} fractal moment is given by:

$$D_q = -\lim_{\delta\to 0}\left[I_q(\delta)/\log(\delta)\right] \qquad \textbf{[37]}$$

In practice, D_q is determined from the slope of the Iq(δ) vs. log δ plot (Hentschel and Procaccia 1983; Appleby 1996). For a 'classic' fractal object, D_q is a simple linear function of q (that is, no addition information is obtained by examining higher moments). For multifractal objects, the relationship between D_q and q is non-linear (**Fig. 14**). Note that D_0 = D is the box-counting dimension (**Sections 3.2, 3.8**), D_1 = σ is the 'information dimension' (**Section 3.9**), and D_2 is the 'correlation dimension' (**Section 3.9**). Negative values of q can be used in multifractal analysis, but the method then becomes very sensitive to grid unit positioning and spatial resolution (Appleby 1996).

Loehle and Wein (1994) argue that scale-specific analyses are required to fully characterize vegetation patterns resulting from the interaction of a number of fractally distributed processes such as soil type, landform and disturbances (see also Scheuring and Riedi 1994). They used a modified version of the generalized entropy method (at q =1) that incorporates the 'degree

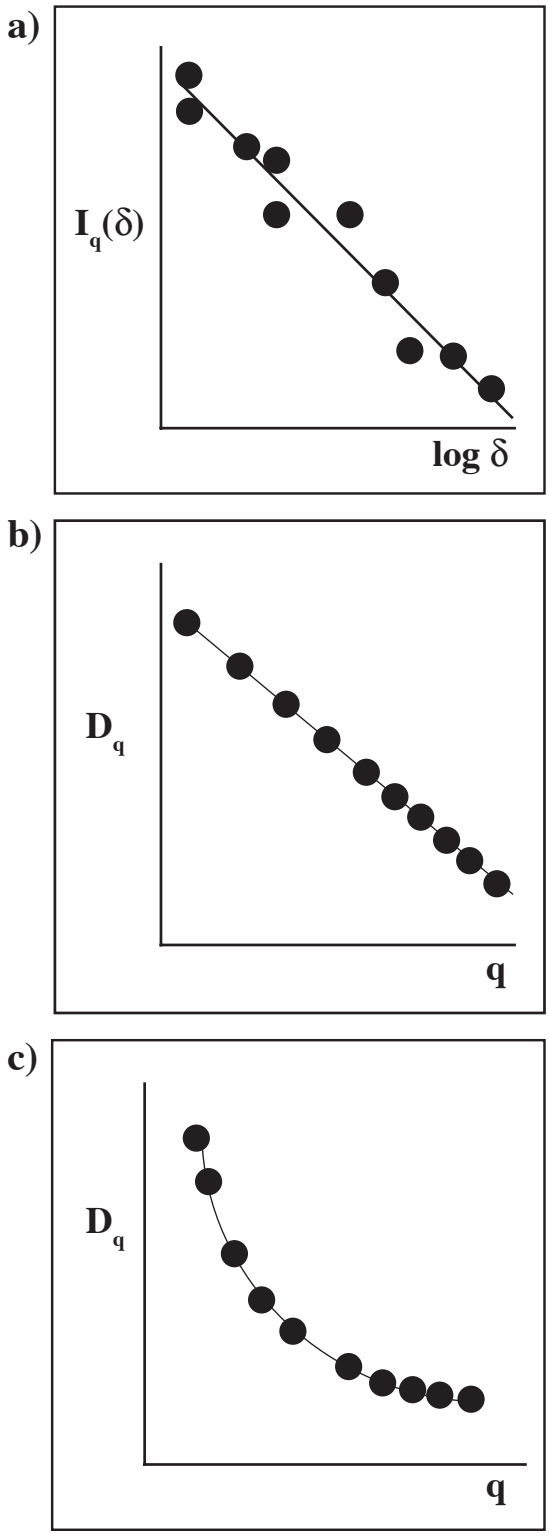

Fig. 14. Multifractals. (a) Plot of Iq(δ) vs. log δ for a given value of q; (b) Linear plot of Dq vs. q indicates a fractal object; (c) Non-linear plot of Dq vs. q indicates a multifractal object.

of similarity' between vegetation classes. This is accomplished by obtaining principal component scores (based on vegetation composition) for each pixel. These component scores are then rescaled into 'probabilities' (deviations from the mean ordination score), and dis-

crete fractal dimensions obtained using:

$$D_{\varepsilon,\gamma} = \frac{\sum_{i=1}^{N\varepsilon} p_i \log p_i \sum_{j=1}^{N\gamma} p_j \log p_j}{\log(1/\varepsilon) - \log(1/\gamma)} \quad \textbf{[38]}$$

where γ is the next larger box size to ε, and Nε is the number of boxes of size ε. Changes in the fractal dimension Dε,γ with changing scale can then be examined (see also Johnson et al. 1995). The method can be criticized on two counts: (a) some information is necessarily lost when principal component scores are substituted for multivariate information; (b) the theoretical basis for rescaling of component scores as 'probabilities' is questionable.

A directly related approach to examining multifractals was suggested by Voss (1988: 66-67). Higher moments of the probability density function (**Section 3.4**) are defined as:

$$M_q(L) = \sum_{n=1}^{N(L)} n_q \rho L \quad \textbf{[39]}$$

At q = 0, the 'configurational entropy' is defined:

$$S(L) = \sum_{n=1}^{N(L)} \log n\rho L \quad \textbf{[40]}$$

For 'classic' fractal objects, all moments give the same value of D. By contrast, multifractal objects have a different value of D for each moment. An example is presented in Voss (1988: 68).

5. APPLICATIONS OF FRACTAL GEOMETRY TO BIOLOGY

5.1 Cell, Protein and Chromosome Structures

Takahashi (1989) hypothesized that the basic architecture of a chromosome is tree-like, consisting of a concatenation of 'mini-chromosomes'. A fractal dimension of D = 2.34 was determined from an analysis of first and second order branching patterns in a human metaphase chromosome. Xu et al. (1994) hypothesized that the twistings of DNA binding proteins have fractal properties.

Lewis and Rees (1985) determined the fractal dimension of protein surfaces ($2 \le D \le 3$) using microprobes. A mean surface dimension of D = 2.4 was determined using microprobe radii ranging from 1-3.5 angstroms. More highly irregular surfaces (D > 2.4) were found to be sites of inter-protein interaction. Wagner et al. (1985) estimated the fractal dimension of heme and iron-sulfur proteins using crystallographic coordinates of the carbon backbone. They found that the structural fractal dimension correlated positively with the temperature dependence of protein relaxation rates.

Smith et al. (1989) used fractal dimension as a measure of contour complexity in two-dimensional images of neural cells. They recommend D as a quantitative morphological measure of cellular complexity.

5.2 DNA Sequences

Self-similarity has recently been found in DNA sequences (summarized in Stanley 1992; see also papers in Nonnenmacher et al. 1994). Glazier et al. (1995) used the multifractal spectrum approach to reconstruct the evolutionary history of organisms from m-DNA sequences. The multifractal spectra for invertebrates and vertebrates were quite different, allowing for the recognition of broad groups of organisms. They concluded that DNA sequences display fractal properties, and that these can be used to resolve evolutionary relationships in animals. Xiao et al. (1995) found that nucleotide sequences in animals, plants and humans display fractal properties. They also showed that exon and intron sequences differ in their fractal properties.

5.3 Enzyme and Ion Channel Kinetics

The kinetics of protein ion channels in the phospholipid bilayer were examined by Liebovitch et al. (1987). The timing of openings and closings of ion channels had fractal properties, implying that processes operating at different time scales are related, not independent (Liebovitch and Koniarek 1992). López-Quintela and Casado (1989) developed a fractal model of enzyme kinetics, based on the observation that kinetics is a function of substrate concentration. They found that some enzyme systems displayed classical Michaelis-Menten kinetics (D = 1), while others showed fractal kinetics (D < 1).

5.4 Dichotomous Branching Systems

Fractal dichotomous branching is seen in the lung, small intestine, blood vessels of the heart, and some neurons (West and Goldberger 1987; Goldberger et al. 1990; Glenny et al. 1991; Deering and West 1992). Fractal branching greatly amplifies the surface area of tissue, be it for absorption (e.g. lung, intestine, leaf mesophyll), distribution and collection (blood vessels, bile ducts, bronchial tubes, vascular tissue in leaves) or information processing (nerves). Fractal structures are

thought to be robust and resistant to injury by virtue of their redundancy and irregularity. Nelson et al. (1990) examined power-law relationships between branch order and length in human, dog, rat and hamster lung tissue. Differences between the human lung and those of other species were hypothesized to be related to postural orientation. Long (1994) relates Leonardo da Vinci's ratio of branch diameters in trees (= 0.707) to observed dichotomous fractal bifurcations.

5.5 Soil Physics

Tyler and Wheatcraft (1990) offer a useful overview of the application of fractal scaling to soil physics. Tyler and Wheatcraft (1989) used particle-size distributions to determine the fractal dimension of various soils, and to relate D to such soil properties as percolation and surface water retention. Perfect and Kay (1991) used a similar method to examine soil fragmentation, while Bartoli et al. (1991) used various methods to estimate the mass, pore and surface fractal dimensions of silty and sandy soils. Eghball et al. (1993) used Rosin's Law to demonstrate that different tillage methods and crop sequences affected soil fragmentation (fractal dimension). Perfect et al. (1993) modelled the relationship between soil aggregate size and tensile strength using a mulifractal approach. Frontier (1987: 340) suggests that it would be interesting to examine the relationship between soil microflora-fauna diversity and soil fractal geometry.

5.6 Plant and Fungal Structures

Vlcek and Cheung (1986) measured the fractal dimension of leaf edges in a number of species. Although D was found to be highly variable in some species (e.g. oaks), they felt that D might have potential as a taxonomic character. The fractal dimension of root systems was examined by Tatsumi et al. (1989) using the box-counting method. They found fractal dimensions in the range 1.46-1.6 for mature crop plants. Fitter and Strickland (1992) demonstrated that the fractal dimension of root systems increases over time (to a maximum of D □ 1.35), and varies between species. Corbit and Garbary (1994) found no differences in the fractal dimension of three algal species, though D increased with both developmental stage and frond structural complexity.

Zeide and Gresham (1991) estimated the fractal dimension of the crown surface of loblolly pine trees in North Carolina, and found evidence that D varies with site quality and thinning intensity. Osawa (1995) determined that trees with higher crown fractal dimensions have less negative self-thinning exponents. It was hypothesized that species-specific changes in foliage packing over time account for this relationship. Chen et al. (1994) developed a fractal-based canopy structure model to calculate light interception in poplar stands.

The fractal geometry of fungal foraging is described by Ritz and Crawford (1990). Fractal dimension varies between fungal species, and tends to be greater when nutrient availability is higher (Bolton and Boddy 1993).

5.7 Chaos and Time Series Analysis

Nonlinear dynamics is the study of systems that respond disproportionately to stimuli. A simple deterministic nonlinear system may behave erratically (though not randomly), a state which has been termed chaos. Chaotic systems are characterized by complex dynamics, determinism, and sensitivity to initial conditions, making long-term forecasting impossible. Chaos, which is closely related to fractal geometry, refers to a kind of constrained randomness (Stone and Ezrati 1996). Wherever a chaotic process has shaped an environment, a fractal structure is left behind.

Goldberger et al. (1990) state that "physiology may prove to be one of the richest laboratories for the study of fractals and chaos as well as other types of nonlinear dynamics". A good example is the study of heart rate time series (Goldberger 1992). Conventional wisdom states that the heart displays 'normal' periodic rhythms that become more erratic in response to stress or age. However, recent evidence suggests just the opposite: physiological processes behave more erratically (chaotically) when they are healthy and young. Normal variation in heart rate is 'ragged' and irregular, suggesting that mechanisms controlling heart rate are intrinsically chaotic. Such a mechanism might offer greater flexibility in coping with emergencies and changing environments. Lipsitz and Goldberger (1992) found a loss of complexity in heart rate variation with age. Based on this result, they defined aging as "a progressive loss of complexity in the dynamics of all physiological systems". Sugihara (1994), using a different analytical approach, found that prediction-decay and nonlinearity models are good predictors of human health. Healthy patients have a steeper heart rate decay curve, and have greater nonlinearity in their heart rhythms. Teich and Lowen (1994) found that human auditory neuron transmissions are best modelled as fractal point processes, and that such transmissions display long-term persistence (H >

0.5). Hahn et al. (1992) examined thermoregulation responses to heat stress in cattle. Fractal dimensions of thermoregulation profiles were found to decrease with increasing stress. They also found that the interval between temperature reading was critical to the detection of changes in thermoregulatory profiles. Similar results were obtained by Escós et al. (1995) in a study of stress in wild goats (spanish ibex). These authors also found that plants under stress show greater variability in allometric relationships, and reduced branch structure complexity.

Basic ideas of chaotic dynamics in population biology are summarized by Schaffer and Kot (1986). The question of whether natural population cycles are deterministic or purely stochastic was examined by Sugihara et al. (1990; also, Sugihara and May 1990). They state that populations are "embedded in a dynamic web of other species and environmental forces", implying that irregularities in population cycles (which have traditionally been 'smoothed' prior to modelling) may provide important information regarding their dynamics. Sugihara et al. (1990) found that for pure additive noise, the correlation of adjacent values was independent of the prediction interval, but for chaotic trends correlations decline as the prediction interval increased. They found that measles epidemics display chaotic properties, but that chickenpox epidemic patterns are best modelled as noise superimposed on a strong annual cycle. Ellner and Turchin (1995) have argued that it is potentially misleading to make a strict distinction between chaotic and stochastic dynamics. Using an approach of non-linear time-series modelling and estimation of Lyapunov exponents (see Godfray and Grenfell 1993), they demonstrated that ecological populations vary from noise-dominated, stable dynamics to weakly chaotic ones. However, Sugihara (1994) claims that their approach is "fundamentally flawed", and offers an alternative method based on locally-weighted maps. Hastings et al. (1993) summarize the various methods available for detecting deterministic chaos in biological time series.

Sugihara and May (1990) examined persistence (probability of extinction) in time series of population sizes. The higher the value of H (lower fractal dimension), the smoother and more persistent the population trend. Higher persistence (H) makes a species more prone to extinction, since population values increase (or decrease) faster over time than in populations having low H. Hastings and Sugihara (1993: 138-160) expand on these ideas, and present examples based on bird and butterfly population time series.

Stone and Ezrati (1996) discuss potential applications of nonlinear dynamics and chaos theory to the study of ecological variability. They argue that chaos theory may be particularly useful in modelling vegetation change, where non-equilibrium dynamics (e.g. disturbance, natural mosaic cycling, and habitat fragmentation) often prevail.

5.8 Organism Size and Number of Individuals

Morse et al. (1985) argued that since habitat has a fractal structure, there will be more 'useable' space for smaller animals than for larger ones. Working with invertebrates, they found that predictions of the number of individuals (by size class) based on body mass and metabolic rate alone consistently underestimated observed field values for the smaller size classes. Predictions were considerably improved when the fractal dimension of the habitat was incorporated into the model: smaller organisms 'perceive' more space and are therefore comparatively more abundant. Shorrocks et al. (1991) confirmed this general result, as did Gunnarsson (1992) and Jeffries (1993) using artificial substrates of differing fractal dimension.

5.9 Movements of Organisms

Fractional Brownian motion models (Frontier 1987: 351-353) have been used to characterize the movement of organisms. Dicke and Burrough (1988) used fractal analysis to examine spider mite movements in the presence and absence of a dispersing pheromone. Wiens and Milne (1989) took a different approach, examining beetle movements in natural fractal landscapes. They found that observed beetle movements deviated from the modelled (fractional Brownian) ones. A follow-up study by Johnson et al. (1992a) found that beetle movements reflect a combination of ordinary (random) and anomalous diffusions. The latter may simply reflect intrinsic departures from randomness, or result from barrier avoidance and utilization of corridors in natural landscapes. Johnson et al. (1992b) discuss the interaction between animal movement characteristics and the patch-boundary features in a 'microlandscape'. They argue that such interactions have important spatial consequences on gene flow, population dynamics and other ecological processes in the community (see also Wiens et al. 1995). In a comparison of path tortuosity in three species or grasshopper, With (1994a) found that the path fractal dimension of the largest species was smaller than those of the two smaller ones. She suggested

that this reflects the fact that smaller species interact with the habitat at a finer scale of resolution than do larger species. In a second study, With (1994b) found differences in the ways that gomphocerine grasshopper nymphs and adults interacted with the microlandscape.

5.10 Ecotone and Interfaces

Frontier (1987: 337-343) discusses the ecological significance of contact zones (ecotonal boundaries) between ecosystems, and outlines how fractal theory can be used to examine boundary phenomena. For example, consider the contact surfaces created by turbulence in aquatic ecosystems (the geometry of which is fractal, Mandelbrot 1982; Milne 1988: 72). Turbulent regions (e.g. interfaces between warm and cold water) have high phytoplankton productivity due to increased contact with resources (nutrients and light), which in turn 'feeds' higher trophic levels. This cascade effect implies that spatial patterns at fine spatial scales determine patterns at broader scales. Pennycuick and Kline (1986) estimated D to determine bald eagle territory sizes along rocky coastlines in Alaska. Forest-grassland ecotones could also be examined in this way to determine habitat available to foraging animals, or to plant species restricted to ecotonal environments. Ecotone concepts can also be applied to the design of public spaces (Arlinghaus and Nystuen 1990).

5.11 Environmental Transects

Burrough (1981) used the semivariogram method to estimate D for various environmental transects (e.g. soil factors, vegetation cover, iron ore content in rocks, rainfall levels, crop yields). He found high fractal dimensions in all cases, from D = 1.4 (iron ore content at 3 m intervals) to D = 2.0 (soil pH at 10 m intervals). Very high fractal dimensions indicate spatial independence of successive values. While some of the series displayed self-similarity over many scales (i.e. a linear log-log plot slope), other trends suggested variation in D with changing scale. Palmer (1988) used the same method to examine spatial dependence of vegetation along transects. Values were generally high but not scale-invariant. Based on a fractal analysis, Phillips (1985) concluded that erosion processes along a portion of the Delaware coast could not be easily predicted.

5.12 Dispersal of Organisms and Disease

Dispersal distances of crop plant pathogens display power-law relationships (van der Plank 1960), and similar relationships have been suggested for plant propagules (Harper 1977). Based on these observations, Kenkel and Irwin (1994) hypothesized that the dispersal of diaspores and pathogens have fractal properties. They suggested that Lévy or Cauchy flights (Mandelbrot 1982: § 32) are appropriate models of dispersal. Species producing diaspores adapted for long-distance dispersal (e.g. 'weeds') have a low fractal dimension. These species advance through the landscape in large leaps, continually establishing new colonies or epicenters (a 'guerilla' strategy). As a result, they display highly patchy distributions at all spatial scales. Conversely, species lacking adaptations for long-distance dispersal move through the landscape more conservatively (a 'phalanx' strategy), with only occasional 'forays' to establish new epicenters. These species have a higher fractal dimension, resulting in less patchy, more continuous spatial distributions. If this model is correct, outbreaks of pathogens having a low fractal dimension will be difficult to predict, since new outbreaks will seem to appear from nowhere.

Shaw (1994) expands on these ideas, noting that classical dispersal probability models are exponential (that is, all their moments are defined). Exponential models assume that dispersal has a characteristic scale, implying that long-distance dispersal is completely negligible. Exponential-based simulation models result in a 'wave-expanding' dispersal pattern, where wave velocity is proportional to the intrinsic population growth rate. However, empirical studies typically demonstrate that gene flows are much greater than those predicted by exponential models. More realistic models are obtained by using dispersal probability distributions having infinite first and higher moments. Shaw (1994, 1995) uses the Cauchy distribution (analogous to the 'Cauchy flight' of Mandelbrot 1982) to model dispersal. Cauchy-based models produce patterns in which 'daughter foci' are continuously formed, so that dispersal is best described as a disjoint set of locations (c.f. Kenkel and Irwin 1993). Mayer and Atzeni (1993) used the Cauchy distribution to model dispersal distance in the screwworm fly.

Wallinga (1995) modelled weed dynamics under the assumption that weed populations are maintained at low densities (through tillage practices, application of herbicides, and so forth). Under such a scenario, populations are expected to display 'critical phenomena' (Grassberger 1983), resulting in their dynamics and spatial pattern being scale-invariant. Fractal analysis (correlation dimension) of a mapped point pattern of cleavers, a

European weed, confirmed the fractal (scale-invariant) nature of weed populations.

Collins and Glenn (1990) argue that competition and dispersal act together to create fractal patterns in tallgrass prairie plant communities. They found evidence of self-similarity in these grasslands (i.e. small-scale patterns are repeated at larger spatial scales).

5.13 Size-Frequency Distributions

The hyperbolic distribution, because it lacks a characteristic scale, describes the sizes of self-similar phenomena (Goodchild and Mark 1987). Meltzer and Hastings (1992) examined the size distribution of grazed areas in Zimbabwe, and related H to the relative stability of vegetation patches. Overall, they found that increases in cattle density decreased patch stability. Using similar methods, Hastings et al. (1982) found lower stability in earlier successional patches. Kent and Wong (1982) used the size-frequency distribution of lakes to estimate the fractal dimension of littoral zone habitat in the Precambrian Shield of Ontario, while Hamilton et al. (1992) estimated terrain fractal dimension based on lake size distributions in the Amazon and Orinoco river floodplains. The hyperbolic distribution has also been fit to taxonomic systems (Burlando 1990, 1993) and the size-distribution of seeds (Hegde et al. 1991). Frontier (1987:359-367) discusses applications of fractal theory to rank-frequency diagrams of the distribution of individuals among species.

5.14 Landscapes

Krummel et al. (1987) examined the fractal dimension of forest patches ('islands') using the perimeter-area method. They found that smaller forest patches had lower mean D than larger patches. The transition zone from low to high fractal dimension occurred at □ 60-73 ha. They concluded that small forest patches are the result of anthropogenic activities. This decrease in landscape complexity with increasing anthropogenic activity was also reported by O'Neill et al. (1988) and Turner and Ruscher (1988). De Cola (1989) used the perimeter-area method to determine fractal dimensions of eight natural and anthropogenic landscape-level classes in northern Vermont. Bian and Walsh (1993) used two-dimensional semivariance to examine scale dependency in the relationship between topography (elevation, slope angle, and slope aspect) and reflectance/absorbance of vegetation at Glacier National Park, Montana. Studies involving fractal dimension estimation of geomorphological features are summarized in Goodchild and Mark (1987), Lam (1990) and Lam and Quattrochi (1992).

5.15 Habitat Complexity and Fragmentation

A simplifying assumption of many classical ecological models is that habitats are uniform, and that they vary linearly with distance. Some recent studies have examined these assumptions and/or modified the classical models in light of the recognized fractal nature of habitats. Scheuring (1991) modified the classical species-area relationship model to include the fractal nature of vegetation. Palmer (1992) modified the 'competition gradient' model of Czárán (1989) to include fractal habitat complexity. He found that species coexistence increased as landscape fractal dimension increased. Milne et al. (1992) examined mammalian herbivore foraging in artificial fractal landscapes. They concluded that the fractal nature of landscapes is an important determinant of resource utilization rates. Milne (1992) examined the fractal geometry of landscapes from the viewpoint of habitat fragmentation. He concluded that habitat fragmentation affects ecosystem processes, and that this must be recognized in developing an ecologically meaningful view of landscapes and habitats. Haslett (1994) found that the fractal dimension of mountain meadow landscapes correlated well with the abundance of syrphid flies, suggesting that more spatial heterogeneous habitats may support more complex ecological communities. Additional potential applications of fractal analysis to vegetation complexity are outlined by van Hees (1994).

5.16 Image and Texture Analysis

The spatial dependency of image elements (e.g. pixels) is referred to as texture. A 'textural feature' is a combination of image elements that cannot be individually differentiated (Musick and Grover 1990). A number of image segmentation methods for the extraction of textural features are available (Davis 1981; van Gool et al. 1985; Blacher et al. 1993). Fractal-based texture methods overcome some of the problems inherent in classical resolution-sensitive techniques (van Gool et al. 1985), and are particularly well-suited to complex natural scenes (Keller et al. 1987; Pentland 1984).

Keller et al. (1989) describe a modified box-counting texture analysis technique based on the probability density function. They characterized simulated (Brodatz) textures in terms of fractal dimension and lacunarity. An alternative box-counting method was proposed by Sarkar and Chaudhuri (1992). In their method, each x,y

coordinate has an associated third dimension (z-coordinate) representing pixel intensity (e.g. gray shade). The box count is determined as the number of cells in a column intercepted by the surface. Using simulated textures, they found that their method was more computationally efficient than that proposed by Keller et. al. (1989); see also Chaudhuri et al. (1993) and Chaudhuri and Sarkar (1995). De Cola (1993) describes a hierarchical grid method for the analysis of surface texture in remotely sensed images. It was found that fractal dimension varied with scale, implying multifractal behaviour.

Pentland (1984) developed a fractional Brownian motion (fBm) approach to image texture analysis based on a modified Fourier algorithm. An analysis of photographs of natural objects found that texture was more effective than spectral properties in characterizing major image features. Keller et al. (1987) used the fBm approach to examine interface complexity of vegetation/landform types. Using the same approach, Dennis and Dessipris (1989) found that anti-aliasing filtering techniques improved estimates of the fractal dimension of 'natural' images, but had little effect on synthetic images.

Image analysis has also been used in medicine and cellular biology. For example, Fortin et al. (1992) analyzed local and large-scale structures in cardiac magnetic resonance images and bone x-rays. They provide detailed descriptions of fBm image analysis models. Note that the methods for fractal analysis of self-affine signals described by Schepers et al. (1992) can also be used in image analysis.

6. CONCLUSIONS

Fractal theory is a unifying concept integrating scale-dependence and complexity, both of which are central to our understanding of biological patterns and processes (West and Goldberger 1987; Wiens 1989; Lam and Quattrochi 1992). Given that fractal and chaos theory are comparatively new fields, it is perhaps not surprising that biologists are still grappling with these concepts. Recognition of the fractal geometry of nature has important implications to biology, as evidenced by the numerous examples presented here. Zeide and Gresham (1991) describe as 'self-evident' the fractal nature of biological structures and systems. We feel that one of the great challenges facing biologists lies in translating these self-evident concepts into comprehensive models of the patterns and processes observed in nature.

ACKNOWLEDGMENTS

Support in the form of Natural Sciences and Engineering Research Council of Canada individual operating grant A-3140 to N.C. Kenkel, and a Heritage Canada (Canadian Parks) research contract to D.J. Walker, are gratefully acknowledged.

REFERENCES

Appleby, S. 1996. Multifractal characterization of the distribution pattern of the human population. Geographical Analysis 28: 147-160.

Arlinghaus, S.L. and J.D. Nystuen. 1990. Geometry of boundary exchanges. Geogr. Rev. 80: 21-31.

Bartoli, F., R. Phillipy, M. Doirisse, S. Niquet and M. Dubuit. 1991. Structure and self-similarity in silty and sandy soils: the fractal approach. J. Soil Sci. 42: 167-185.

Bian, L. and S.J. Walsh. 1993. Scale dependencies of vegetation and topography in a mountainous environment of Montana. Prof. Geogr. 45: 1-11.

Blacher, S., F. Brouers and R. Van Dyck. 1993. On the use of fractal concepts in image analysis. Physica A. 197: 516 - 527.

Bolton, R.G. and L. Boddy. 1993. Characterization of the spatial aspects of foraging mycelial cord systems using fractal geometry. Mycol. Res. 97: 762-768.

Brown, S.R. 1995. Measuring the dimension of self-affine fractals: examples of rough surfaces. In: C.C. Barton and P.R. La Pointe (eds.). Fractals in the earth sciences. pp. 77-87. Plenum Press, New York.

Burlando, B. 1990. The fractal dimension of taxonomic systems. J. Theor. Biol. 146: 99-114.

Burlando, B. 1993. The fractal geometry of evolution. J. Theor. Biol. 163: 161-172.

Burrough, P.A. 1981. Fractal dimensions of landscapes and other environmental data. Nature 294: 240-242.

Burrough, P.A. 1983. Multiscale sources of spatial variation in soil. I. The application of fractal concepts to nested levels of soil variation. J. Soil Sci. 34: 577-597.

Burrough, P.A. 1986. Principles of geographical systems for land resources assessment. Clarendon, Oxford.

Chaudhuri, B.B. and Sarkar, N. 1995. Texture segmentation using fractal dimension. IEEE Trans. Pattern Anal. Machine Intelligence. 17: 72 - 77.

Chaudhuri, B.B., N. Sarkar and P. Kundu. 1993. Improved fractal geometry based texture segmentation technique. IEE Proc. E, Comp. Digital Tech. 140: 233 - 241.

Chen, S.G., R. Ceulemans and I. Impens. 1994. A fractal-based Populus canopy structure model for the calculation of light interception. For. Ecol. Manage. 69: 97-102.

Collins, S.L. and S.M. Glenn. 1990. A hierarchical analysis of species' abundance patterns in grassland vegetation. Am. Nat. 135: 633-648.

Corbit, J.D. and D.J. Garbary. 1995. Fractal dimension as a quantitative measure of complexity in plant development. Proc. R. Soc. Lond. B 262: 1-6.

Crawford, J.W. and I.M. Young. 1990. A multiple scaled fractal tree. J. Theor. Biol. 145: 199-206.

Curran, P.J. 1988. The semivariogram in remote sensing: an introduction. Remote Sens. Envir. 24: 493-507.

Czárán, T. 1989. Coexistence of competing populations along environmental gradients: a simulation study. Coenoses 4: 113-120.

Davis, L.S. 1980. Image texture analysis techniques - a survey. In: J.C. Simon and R.M. Haralick (eds.). Digital image processing. pp. 189-201. D. Reidel Publishing, Dordrecht, Netherlands.

De Cola , L. 1993. Multifractals in image processing and process imaging. In: Lam, N.S. and L. De Cola (eds.). Fractals in geography. pp. 282-304. Prentice Hall, Englewood Cliffs, NJ, U.S.A.

De Cola, L. 1989. Fractal analysis of a classified Landsat scene. Photogram. Eng. Remote Sens. 55: 601-610.

De Cola, L. 1991. Fractal analysis of multiscale spatial autocorrelation among point data. Envir. Plan. A 23: 545-556.

Deering, W. and B.J. West. 1992. Fractal physiology. IEEE Engin. Med. Biol. 11: 40-46.

Dennis, T.J. and N.G. Dessipris. 1989. Fractal modeling in image texture analysis. IEE Proc. F Radar Signal Process. 136: 227 - 235.

Dicke, M. and P.A. Burrough. 1988. Using fractal dimensions for characterizing tortuosity of animal trails. Physiol. Entom. 13: 393-398.

Eghball, B., L.N. Mielke, G.A. Calvo and W.W. Wilhelm. 1993. Fractal description of soil fragmentation for various tillage methods and crop sequences. Soil Sci. Soc. Am. J. 57: 1337-1341.

Ellner, S. and P. Turchin. 1995. Chaos in a noisy world: new methods and evidence from time-series analysis. Amer. Nat. 145: 343-375.

Escos, J.M., C.L. Alados and J.M. Emlen. 1995. Fractal structures and fractal functions as disease indicators. Oikos 74: 310-314.

Falconer, K. 1990. Fractal geometry. Mathematical foundations and applications. J. Wiley and Sons, New York.

Farmer, J.D., E. Ott and J.A. Yorke. 1983. The dimension of chaotic attractors. Physica 7D: 153-180.

Fitter, A.H. & T.R. Strickland. 1992. Fractal characterization of root system architecture. Funct. Ecol. 6: 632-635.

Fortin, C., R. Kumaresan, W. Ohley and S. Hoefer. 1992. Fractal dimension in the analysis of medical images. IEEE Eng. Med. Biol. 11: 65-71.

Frontier, S. 1987. Applications of fractal theory to ecology. In: Legendre, P. & L. Legendre (eds). Developments in numerical ecology. pp. 335-378. Springer, Berlin.

Gautestad, A.O. and I. Mysterud. 1994. Fractal analysis of population ranges: methodological problems and challenges. Oikos 69: 154-157.

Glazier, J.A., S. Raghavachari, C.L. Berthlesen and M.H. Skolnick. 1995. Reconstructing phylogeny from the multifractal spectrum of mitochondrial DNA. Physical Review E 51: 2665-2668.

Glenny, R.W., H.T. Robertson, S. Yamashiro and J.B. Bassingthwaighte. 1991. Applications of fractal analysis to physiology. J. Appl. Physiol. 70: 2351-2367.

Godfray, H.C.J. and B.T. Grenfell. 1993. The continuing quest for chaos. Trends Ecol. Evol. 8: 43-44.

Goldberger, A.L. 1992. Fractal mechanisms in the electrophysiology of the heart. IEEE Eng. Medicine Biol. 11: 47-52.

Goldberger, A.L., D.G. Rigney and B.J. West. 1990. Chaos and fractals in human physiology. Sci. Am. 262(2): 42-49.

Goodchild, M.F. & D.M. Mark. 1987. The fractal nature of geographic phenomena. Ann. Assoc. Amer. Geogr. 77: 265-278.

Goodchild, M.F. 1980. Fractals and the accuracy of geographical measures. Math. Geogr. 12: 85-98.

Grassberger, P. 1983. On the critical behavior of the general epidemic process and dynamical percolation. Math. Biosci. 63: 157-162.

Grassberger, P. and I. Procaccia. 1983. Characterization of strange attractors. Phys. Rev. Letters 50: 346-349.

Gunnarsson, B. 1992. Fractal dimension of plants and body size distribution in spiders. Funct. Ecol. 6: 636-641.

Hahn, G.L., Y.R. Chen, J.A. Nienaber, R.A. Eigenberg and A.M. Parkhurst. 1992. Characterizing animal stress through fractal analysis of thermoregulatory responses. J. Therm. Biol. 17: 115-120.

Hamilton, S.K., J.M. Melack, M.F. Goodchild and W.M. Lewis. 1992. Estimation of the fractal dimension of terrain from lake size distributions. In: P.A. Carling and G.E. Petts (eds.). Lowland floodplain rivers: geomorphological perspectives. pp. 145-163. J. Wiley and Sons, New York.

Harper, J.L. 1977. Population biology of plants. Academic Press, New York.

Haslett, J.R. 1994. Community structure and the fractal dimensions of mountains habitats. J. Theor. Biol. 167: 407-411.

Hastings, A., C.L. Hom, S. Ellner, P. Turchin and H.C.J. Godfray. 1993. Chaos in ecology: is mother nature a strange attractor? Ann. Rev. Ecol. Syst. 34: 1-33.

Hastings, H.M. and G. Sugihara. 1993. Fractals: a user's guide for the natural sciences. Oxford University Press, Oxford, England.

Hastings, H.M., B.S. Schneider, M.A. Schreiber, K. Gorray, G. Maytal and J. Maimon. 1992. Statistical geometry of pancreatic islets. Proc. Royal Soc. London B 250: 257-261.

Hastings, H.M., R. Pekelney, R. Monticciolo, D. Vun Kannon & D. Del Monte. 1982. Time scales, persistence and patchiness. Biosyst. 15: 281-289.

Hegde, S.G., R. Lokesha & K.N. Ganeshaiah. 1991. Seed size distribution in plants: an explanation based on fractal geometry. Oikos 62: 100-101.

Hentschel, H.G.E. and I. Procaccia. 1983. The infinite number of generalized dimensions of fractals and strange attractors. Physica 8D: 435-444.

Huang, J. and D.L. Turcotte. 1989. Fractal mapping of digitized images: application to the topography of Arizona and comparisons with synthetic images. J. Geophys. Res. 94: 7491-7495.

Hurst, H.E. 1951. Long-term storage capacity of reservoirs. Trans. Am. Soc. Civil Eng. 116: 770-808.

Jeffries, M. 1993. Invertebrate colonization of artificial pondweeds of differing fractal dimension. Oikos 67: 142-148.

Johnson, A.R., B.T. Milne and J.A. Wiens. 1992a. Diffusion in fractal landscapes: simulations and experimental studies of tenebrionid beetle movements. Ecology 73: 1968-1983.

Johnson, A.R., J.A. Wiens, B.T. Milne and T.O. Crist. 1992b. Animal movements and population dynamics in heterogeneous landscapes. Land. Ecol. 7: 63-75.

Johnson, G.D., A. Tempelmand G.P. Patil. 1995. Fractal based methods in ecology: a review for analysis at multiple spatial scales. Coenoses 10: 123-131.

Katz, M.J. 1988. Fractals and the analysis of waveforms. Comput. Biol. Med. 18: 145-156.

Keller, J.M., R. M. Crownover and R.Y. Chen. 1987. Characteristics of natural scenes related to the fractal dimension. IEEE Trans. Pattern Anal. Mach. Intelligence. 9: 621 - 627.

Keller, J.M., S. Chen and R.M. Crownover. 1989. Texture description and segmentation through fractal geometry. Comp. Vision Graph. Image Process. 45: 150-166.

Kenkel, N.C. and A.J. Irwin. 1994. Fractal analysis of dispersal. Abst. Bot. 18: 79-84.

Kenkel, N.C. and D.J. Walker. 1993. Fractals and ecology. Abst. Bot. 17: 53-70.

Kent, C. & J. Wong. 1982. An index of littoral zone complexity and its measurement. Can. J. Fish. Aquat. Sci. 39: 847-853.

King, R.B., L.J. Weissman & J.B. Bassingthwaighte. 1989. Fractal descriptions for spatial statistics. Ann. Biomed. Eng. 18: 111-122.

Klinkenberg, B. 1993. A review of methods used to determine the fractal dimension of linear features. Math. Geol. 25: 1003-1026.

Krummel, J.R., R.H. Gardner, G. Sugihara, R.V. O'Neill & P.R. Coleman. 1987. Landscape patterns in a disturbed environment. Oikos 48: 321-324.

Lam, N. S. and L. De Cola (eds.). 1993. Fractals in geography. Prentice Hall, Englewood Cliffs, NJ, U.S.A.

Lam, N.S. 1990. Description and measurement of Landsat TM images using fractals. Photogram. Eng. Remote Sens. 56: 187-195.

Lam, N.S. and D.A. Quattrochi. 1992. On the issues of scale, resolution, and fractal analysis in the mapping sciences. Prof. Geogr. 44: 88-98.

Leduc, A., Y.T. Prairie and Y. Bergeron. 1994. Fractal dimension estimates of a fragmented landscape: sources of variability. Land. Ecol. 9: 279-286.

Lee, C.-K. and S.-L. Lee. 1995. Multifractal scaling analysis of reactions over fractal surfaces. Surface Sci. 325: 294-310.

Lewis, M. and D.C. Rees. 1985. Fractal surfaces of proteins. Science 230: 1163-1165.

Liebovitch, L.S. and J.P. Koniarek. 1992. Ion channel kinetics. Protein switching between conformational states is fractal in time. IEEE Eng. Medicine Biol. 11: 53-56.

Liebovitch, L.S., J. Fischbarg and J.P. Koniarek. 1987. Ion channel kinetics: a model based on fractal scaling rather than multistate Markov processes. Math. Biosci. 84: 37-68.

Lipsitz, L.A. and A.L. Goldberger. 1992. Loss of 'complexity' and aging. J. Am. Med. Assoc. 267: 1806-1809.

Loehle, C. 1983. The fractal dimension and ecology. Specul. Sci. Tech. 6: 131-142.

Loehle, C. and G. Wein. 1994. Landscape habitat diversity: a multiscale information theory approach. Ecol. Modeling 73: 311-329.

Loehle, C. and L. Bai-Lian. 1996. Statistical properties of ecological and geologic fractals. Ecol. Modeling 85: 271-284.

Long, C.A. 1994. Leonardo da Vinci's rule and fractal complexity in dichotomous trees. J. Theor. Biol. 167: 107-113.

Longley, P.A. and M. Batty. 1989. On the fractal measurement of geographical boundaries. Geogr. Anal. 21: 47-67.

López-Quintela, M.A. and J. Casado. 1989. Revision of the methodology in enzyme kinetics: a fractal approach. J. Theor. Biol. 139: 129-139.

Lorimer, N.D., R.G. Haight and R.A. Leary. 1994. The fractal forest: fractal geometry and applications in forest science. U.S. Department of Agriculture, Forest Service. North Central Forest Experimental Station, General Technical Report NC-170. 43 pages.

Mandelbrot, B.B. 1967. How long is the coastline of Britain? Statistical self-similarity and fractional dimension. Science 156: 636-638.

Mandelbrot, B.B. 1975. Stochastic models for the Earth's relief, the shape and the fractal dimension of the coastlines, and the number-area rule for islands. Proc. Nat. Acad. Sci. U.S.A. 72: 3825-3828.

Mandelbrot, B.B. 1982. The fractal geometry of nature. Freeman, San Francisco.

Mandelbrot, B.B., D.E. Passaja and A.T. Paulley. 1984. Fractal character of fractal surfaces of metals. Nature (London) 308: 721-722.

Mayer, D.G. and M.G. Atzeni. 1993. Estimation of dispersal distances for Cochliomyia hominivorax (Diptera: Calliphoridae). Environ. Entomol. 22: 368-374.

Meltzer, M.I. and H.M. Hastings. 1992. The use of fractals to assess the ecological impact of increased cattle population: case study from the Runde Communal Land, Zimbabwe. J. Appl. Ecol. 29: 635-646.

Milne, B. 1991b. The utility of fractal geometry in landscape design. Landscape and Urban Planning 21: 81-90.

Milne, B.T. 1988. Measuring the fractal geometry of landscapes. Appl. Math. Comp. 27: 67-79.

Milne, B.T. 1991a. Lessons from applying fractal models to landscape patterns. In: Turner, M.G. & R.H. Gardner (eds). Quantitative methods in landscape ecology: the analysis and interpretation of landscape heterogeneity. pp. 199-235. Springer-Verlag, New York.

Milne, B.T. 1992. Spatial aggregation and neutral models in fractal landscapes. Am. Nat. 139: 32-57.

Milne, B.T., M.G. Turner, J.A. Wiens and A.R. Johnson. 1992.

Interactions between the fractal geometry of landscapes and allometric herbivory. Theor. Pop. Biol. 41: 337-353.

Morse, D.R., J.H. Lawton, M.M. Dodson & M.H. Williamson. 1985. Fractal dimension of vegetation and the distribution of arthopod body lengths. Nature 314: 731-733.

Musick, H.B. & H.D. Grover. 1990. Image textural measures as indices of landscape pattern. In: Turner, M.G. and R.H. Gardner (eds.). Quantitative methods in landscape ecology. pp. 77-103. Springer-Verlag, New York.

Nelson, T.R., B.J. West and A.L. Goldberger. 1990. The fractal lung: universal and species-related scaling patterns. Experimentia 46: 251-254.

Niklas, K.J. 1994. Plant allometry. The scaling of form and process. University of Chicago Press, Chicago.

Nonnenmacher, T.F., G.A. Losa and E.R. Weibel. 1994. Fractals in biology and medicine. Birkhäuser, Cambridge.

Normant, F. and C. Tricot. 1991 (eds.). Methods for evaluating the fractal dimension of curves using convex hulls. Phys. Rev. A 43: 6518-6525.

Normant, F. and C. Tricot. 1993. Fractal simplification of lines using convex hulls. Geogr. Anal. 25: 118-129.

O'Neill, R.V., J.R. Krummel, R.H. Gardner, G. Sugihara, B. Jackson, D.L. DeAngelis, B.T. Milne, M.G. Turner, B. Zygmunt, S.W. Christensen, V.H. Dale and R.L. Graham. 1988. Indices of landscape pattern. Land. Ecol. 1: 153-162.

Ogata, Y. and K. Katsura. 1991. Maximum likelihood estimates of the fractal dimension for random spatial patterns. Biometrika 78: 463-474.

Olsen, E.R., R.D. Ramsey and D.S. Winn. 1993. A modified fractal dimension as a measure of landscape diversity. Photogram. Eng. Remote Sens. 59: 1517-1520.

Osawa, A. 1995. Inverse relationship of crown fractal dimension to self-thinning exponent of tree populations: a hypothesis. Can. J. For Res. 25: 1608-1617.

Palmer, M.W. 1988. Fractal geometry: a tool for describing spatial patterns of plant communities. Vegetatio 75: 91-102.

Palmer, M.W. 1992. The coexistence of species in fractal landscapes. Am. Nat. 139: 375-397.

Peitgen, H.-O., H. Jürgens and D. Saupe. 1992. Fractals for the classroom. Springer, New York.

Pennycuick, C.J. and N.C. Kline. 1986. Units of measurement for fractal extent, applied to the coastal distribution of bald eagle nests in the Aleutian islands, Alaska. Oecologia (Berlin) 68: 254-258.

Pentland, A.P. 1984. Fractal-based description of natural scenes. IEEE Trans. Pattern Anal. Machine Intelligence. 6: 661 - 674.

Perfect, E. and B.D. Kay. 1991. Fractal theory applied to soil aggregation. Soil Sci. Soc. Am. J. 55: 1552-1558.

Perfect, E., B.D. Kay and V. Rasiah. 1993. Multifractal model for soil aggregate fragmentation. Soil Sci. Soc. Am. J. 57: 896-900.

Perfect, E., V. Rasiah and B.D. Kay. 1992. Fractal dimension of soil aggregate-size distributions calculated by number and mass. Soil Sci. Soc. Am. J. 56: 1407-1409.

Peters, E.E. 1994. Fractal market analysis. Applying chaos theory to investment and economics. J. Wiley and Sons, New York.

Phillips, J.D. 1985. Measuring complexity of environmental gradients. Vegetatio 64: 95-102.

Polidori, L., J.J. Chorowicz and R. Guillande. 1991. Description of terrain as a fractal surface, and application to digital elevation model quality assessment. Photogramm. Engin. Remote Sens. 57: 1329-1332.

Pruess, S.A. 1995. Some remarks on the numerical estimation of fractal dimension. In: C.C. Barton and P.R. La Pointe (eds.). Fractals in the earth sciences. pp. 65-75. Plenum Press, New York.

Rényi, A. 1970. Probability theory. North-Holland, Amsterdam.

Rieu, M. and G. Sposito. 1991a. Fractal fragmentation, soil porosity, and soil water properties: I. Theory. Soil Sci. Soc. Am. J. 55: 1231-1238.

Rieu, M. and G. Sposito. 1991b. Fractal fragmentation, soil porosity, and soil water properties: II. Applications. Soil Sci. Soc. Am. J. 55: 1239-1244.

Ritz, K. and J. Crawford. 1990. Quantification of the fractal nature of colonies of Trichoderma viride. Mycol. Res. 94: 1138-1152.

Robertson, M.C. and C.G. Sammis. 1995. Fractal analysis of three-dimensional spatial distributions of earthquakes with a percolation interpretation. J. Geophys. Res. 100: 609-620.

Roy, A.G., G. Gravel and C. Gauthier. 1987. Measuring the dimension of surfaces: a review and appraisal of different methods. Proceedings, 8th International Symposium on Computer-Assisted Cartography (Auto-Carto 8), Baltimore, U.S.A. pp. 68-77.

Russell, R.W., G.L. Hunt, K.O. Coyle and R.T. Cooney. 1992. Foraging in a fractal environment: spatial patterns in a marine predator-prey system. Land. Ecol. 7: 195-209.

Sarkar, N. and B.B. Chaudhuri. 1992. An efficient approach to estimate fractal dimension of textural images. Pattern Recog. 25: 1035 - 1041.

Schaffer, W.M. and M. Kot. 1986. Chaos in ecological systems: the coals that Newcastle forgot. Trends Ecol. Evol. 1: 58-63.

Schepers, H.E., J.H.G.M. van Beek and J.B. Bassingthwaighte. 1992. Four methods to estimate the fractal dimension from self-affine signals. IEEE Eng. Med. Biol. 11: 57-64.

Scheuring, I. 1991. The fractal nature of vegetation and the species-area relation. Theor. Popul. Biol. 39: 170-177.

Scheuring, I. and R.H. Riedi. 1994. Application of multifractals to the analysis of vegetation pattern. J. Veg. Sci. 5: 489-496.

Schroeder, M. 1991. Fractals, chaos, power laws. Minutes from an infinite paradise. Freeman, New York.

Shaw, M.W. 1994. Modeling stochastic processes in plant pathology. Annu. Rev. Phytopathol. 32: 523-544.

Shaw, M.W. 1995. Simulation of population expansion and spatial pattern when individual dispersal distributions do not decline exponentially with distance. Proc. Royal Soc. London B 259: 243-248.

Shorrocks, B., J. Marsters, I. Ward & P.J. Evennett. 1991. The fractal dimension of lichens and the distribution of arthropod

body lengths. Funct. Ecol. 5: 457-460.

Smith, T.G., W.B. Marks, G.D. Lange, W.H. Sheriff and E.A. Neale. 1989. A fractal analysis of cell images. J. Neurosci. Meth. 27: 173-180.

Stanley, H.E. 1992. Fractal landscapes in physics and biology. Physica A 186: 1-32.

Stanley, H.E. and P. Meakin. 1988. Multifractal phenomena in physics and chemistry. Nature 335: 405-409.

Stone, L. and S. Ezrati. 1996. Chaos, cycles and spatiotemporal dynamics in plant ecology. J. Ecol. 84: 279-291.

Sugihara, G. & R.M. May. 1990. Applications of fractals in ecology. Trends Ecol. Evol. 5: 79-86.

Sugihara, G. 1994. Nonlinear forecasting for the classification of natural time series. Phil. Trans. R. Soc. Lond. A: 477-495.

Sugihara, G., B. Grenfell and R.M. May. 1990. Distinguishing error from chaos in ecological time series. Phil. Trans. R. Soc. London B 330: 235-251.

Takahashi, M. 1989. A fractal model of chromosomes and chromosomal DNA replication. J. Theor. Biol. 141: 117-136.

Tatsumi, J., A. Yamauchi and Y. Kono. 1989. Fractal analysis of plant root systems. Ann. Bot. 64: 499-503.

Taylor, C.C. and S.J. Taylor. 1991. Estimating the dimension of a fractal. J. R. Statist. Soc. B 53: 353-364.

Taylor, R.A.J. 1988. A fractal approach to analysis of tree ring increments. U.S. Department of Agriculture, Forest Service, Southern Forest Experimental Station, General Technical Report SO-69. New Orleans, LA, U.S.A. pp. 40-56.

Teich, M.C. and S.B. Lowen. 1994. Fractal patterns in auditory nerve-spike trains. IEEE Eng. Med. Biol. 13: 197-202.

Tricot, C. 1991. Curves and fractal dimension. Springer-Verlag, New York.

Tsonis, A.A. and P.A. Tsonis. 1987. Fractals: a new look at biological shape and patterning. Persp. Biol. Med. 30: 355-361.

Turcotte, D.L. 1986. Fractals and fragmentation. J. Geophys. Res. 91: 1921-1926.

Turcotte, D.L. 1992. Fractals and chaos in geology and geophysics. Cambridge University Press, Cambridge, England.

Turner, M.G. & C.L. Ruscher. 1988. Changes in landscape patterns in Georgia, USA. Land. Ecol. 1: 241-251.

Tyler, S.W. and S.W. Wheatcraft. 1989. Application of fractal mathematics to soil water retention estimation. Soil Sci. Soc. Amer. J. 53: 987-996.

Tyler, S.W. and S.W. Wheatcraft. 1990. The consequences of fractal scaling in heterogeneous soils and porous media. In: Hillel, D. and E. Elrick (editors). Scaling in soil physics. Principles and applications. pp. 109-122. Soil Sci. Soc. Amer. Special Pul. 25. Madison, WI, USA.

van der Plank, J.E. 1960. Analysis of epidemics. In: Horsfall, J.G. and A.E. Dimond (eds.). Plant pathology, an advanced treatise. Vol. 3. The diseased population, epidemics and control. pp. 230-289. Academic Press, New York.

Van Gool, L., P. Dewaele and A. Oosterlinck. 1985. Texture analysis anno 1983. Comput. Vision Graphics Image Process. 29: 336 - 357.

van Hees, W.W.S. 1994. A fractal model of vegetation complexity in Alaska. Land. Ecol. 9: 271-278.

Virkkala, R. 1993. Ranges of northern forest passerines: a fractal analysis. Oikos 67: 218-226.

Vlcek, J. and E. Cheung. 1986. Fractal analysis of leaf shapes. Can. J. For. Res. 16: 124-127.

Voss, R.F. 1988. Fractals in nature: from characterization to simulation. In: Peitgen, H.-O. and D. Saupe (eds.). The science of fractal images. pp. 21-70. Springer, New York.

Wagner, G.C., J.T. Colvin, J.P. Allen and H.J. Stapleton. 1985. Fractal models of protein structure, dynamics and magnetic relaxation. J. Am. Chem. Soc. 107: 5589-5594.

Wallinga, J. 1995. The role of space in plant population dynamics: annual weeds as an example. Oikos 74: 377-383.

West, B.J. and A.L. Goldberger. 1987. Physiology in fractal dimensions. Am. Sci. 75: 354-365.

Wiens, J.A. 1989. Spatial scaling in ecology. Funct. Ecol. 3: 385-397.

Wiens, J.A. and B.T. Milne. 1989. Scaling of 'landscapes' in landscape ecology, or landscape ecology from a beetle's perspective. Land. Ecol. 3: 87-96.

Wiens, J.A., T.O. Crist, K.A. With and B.T. Milne. 1995. Fractal patterns of insect movement in microlandscape mosaics. Ecology 76: 663-666.

Williamson, M.H. and J.H. Lawton. 1991. Measuring habitat structure with fractal geometry. In: Bell, S., E.D. McCoy and H.R. Mushinsky (eds.). Habitat structure: the physical arrangement of objects in space. pp. 69-86. Chapman and Hall, London.

With, K.A. 1994a. Using fractal analysis to assess how species perceive landscape structure. Land. Ecol. 9: 25-36.

With, K.A. 1994b. Ontogenetic shifts in how grasshoppers interact with landscape structure: an analysis of movement patterns. Funct. Ecol. 8: 477-485.

Xiao, Y., R. Chen, R. Shen, J. Sun and J. Xu. 1995. Fractal dimension of exon and intron sequences. J. Theor. Biol. 175: 23-26.

Xu, J., Y. Chao and R. Chen. 1994. Fractal geometry study of DNA binding proteins. J. Theor. Biol. 171: 239-249.

Zeide, B. & C.A. Gresham. 1991. Fractal dimensions of tree crowns in three loblolly pine plantations of coastal South Carolina. Can. J. For. Res. 21: 1208-1212.

Zeide, B. 1991. Fractal geometry in forestry applications. For. Ecol. Manage. 46: 179-188.

Zeide, B. and P. Pfeifer. 1991. A method for estimation of fractal dimension of tree crowns. For. Sci. 37: 1253-1265.